

Drought risk under climate and land use changes: implication to water resource availability at catchment scale

Article

Published Version

Creative Commons: Attribution 4.0 (CC-BY)

Open Access

Afzal, M. and Ragab, R. (2019) Drought risk under climate and land use changes: implication to water resource availability at catchment scale. *Water*, 11 (9). 1790. ISSN 2073-4441 doi: 10.3390/w11091790 Available at <https://centaur.reading.ac.uk/85974/>

It is advisable to refer to the publisher's version if you intend to cite from the work. See [Guidance on citing](#).

To link to this article DOI: <http://dx.doi.org/10.3390/w11091790>

Publisher: MDPI

All outputs in CentAUR are protected by Intellectual Property Rights law, including copyright law. Copyright and IPR is retained by the creators or other copyright holders. Terms and conditions for use of this material are defined in the [End User Agreement](#).

www.reading.ac.uk/centaur

CentAUR

Central Archive at the University of Reading

Reading's research outputs online

Article

Drought Risk under Climate and Land Use Changes: Implication to Water Resource Availability at Catchment Scale

Muhammad Afzal ^{1,2,*} and Ragab Ragab ²¹ School of Earth and Ocean Sciences, Cardiff University, Main Building, Park Place, Cardiff CF10 3AT, UK² Centre for Ecology & Hydrology (CEH), Wallingford, Oxfordshire OX10 8BB, UK

* Correspondence: AfzalM8@cardiff.ac.uk

Received: 10 July 2019; Accepted: 24 August 2019; Published: 28 August 2019



Abstract: Although the climate change projections are produced by global models, studying the impact of climatic change on water resources is commonly investigated at catchment scale where the measurements are taken, and water management decisions are made. For this study, the Frome catchment in the UK was investigated as an example of midland England. The DiCaSM model was applied using the UKCP09 future climate change scenarios. The climate projections indicate that the greatest decrease in groundwater recharge and streamflow was projected under high emission scenarios in the 2080s. Under the medium and high emission scenarios, model results revealed that the frequency and severity of drought events would be the highest. The drought indices, the Reconnaissance Drought Index, RDI, Soil Moisture Deficit, SMD and Wetness Index, WI, predicted an increase in the severity of future drought events under the high emission scenarios. Increasing broadleaf forest area would decrease streamflow and groundwater recharge. Urban expansion could increase surface runoff. Decreasing winter barley and grass and increasing oil seed rape, would increase SMD and slightly decrease river flow. Findings of this study are helpful in the planning and management of the water resources considering the impact of climate and land use changes on variability in the availability of surface and groundwater resources.

Keywords: DiCaSM hydrological model; climate change scenarios; land use change; Frome catchment; catchment water balance

1. Introduction

Changes in the land surface hydrology are attributed to the multiple effects of the changes in climate, vegetation, and soil [1]. Therefore, it is important to understand the combined impact of climate and land use changes on water resource availability. Drought has significant economic, social and ecological impacts; however, there is no universal consensus about the definition of drought [2]. Commonly, drought occurs due to an extended period receiving below average rainfall. This is considered a meteorological drought, which progresses into agricultural, hydrological, and socio-economic drought [3]. The general perception is that the UK is not a drought-prone country; however, the UK has experienced frequent occurrence of drought events such as those of the 1970s, 1980s and 1990s, where summer drought events were the outcome of increased variability in climate [4]. These events were followed by another severe drought event that occurred in 1995, mainly affecting the north and western parts of the country [5]. The UK also experienced a severe drought in 2006 which took place in large parts of Southern Britain as a result of two successive dry winter and spring periods, followed by a hot and dry summer [6]. Most recently, the entire UK experienced a drought period in 2018. However, the 1970s drought was considered the most serious of the past century in the south-east of England, during which eight water companies introduced hosepipe bans that affected

15.6 million people and placed water consumers under intense scrutiny [7]. Another significant drought event that affected most parts of England and Wales was the 2010–2012 drought, ranked as the most significant one- to two-year drought in lowland England in the last 100 years [8]. Rainfall deficiency was disproportionally concentrated in the spring, autumn and winter seasons when normally the bulk of the replenishment of reservoirs and underground aquifers takes place. Also, during this period, wetter spells that took place during the summer months did not make a difference to water resources due to the high soil moisture deficit caused by high water losses by evapotranspiration.

In the UK, reservoirs refill and groundwater is replenished during the November–April period when evaporation losses are minimal. A decrease in the rainfall, more particularly during the spring months, would put water supplies under pressure, particularly the lowlands of the country where groundwater is the principal source of water supplies [6]. The severity of drought events of recent years suggest an increased likelihood of these events in the future. The modelling study predicted an increase in temperature which will result in drier summers and wetter winters, and that would likely cause a reduction in water resource availability [9]. Climate change could have significant impacts on water supply systems and this is of more concern for England and Wales where the groundwater accounts for over 35% of the water supply [10]. Although a number of historical drought events have been studied across the UK [4,5,11–14], they have mainly focused on the events themselves, while less attention has been given to finding a number of drought indices which could represent all meteorological, hydrological and agricultural droughts under current and future climatic/land use change. Although some of the studies applied a modelling approach to study the severity of future droughts, a little work has been done to study the impacts of climate change on the drought at catchment scale under current and future climate and land use change scenarios. This is the aim of the current study.

2. Study Area, Data and Methodology

2.1. Study Area

The catchment of the River Frome (National River Flow Archive (NRFA) reference 53006) was selected for this study. It is in south Gloucestershire, in the South West Region of the UK; the catchment's area is 148.9 km². The River Frome flows in a south westerly direction towards Bristol and the gauging station is at Frenchay (Figure 1). The mean annual rainfall of the catchment is around 792 mm, and the river flow is dominated by rapid surface runoff [15]. The studied catchment is of complex geology, as the eastern and central parts of the catchment are dominated by sandstone of the Coal Measures and Mercia Mudstone, while west of the catchment is less permeable. Superficial deposits are meltwater gravels and terraces, mainly in the west. The main land use practices of the catchment are grass land, crops and urban development (Figure 2). A more detailed land use is given in Figure 3: 36% of the catchment area is grassland, 23% is urban, 9% winter wheat, 12% spring barley, 10% winter barley, 3% forest, 4% other cereals, 1% potato, 2% bare soil and other crops.

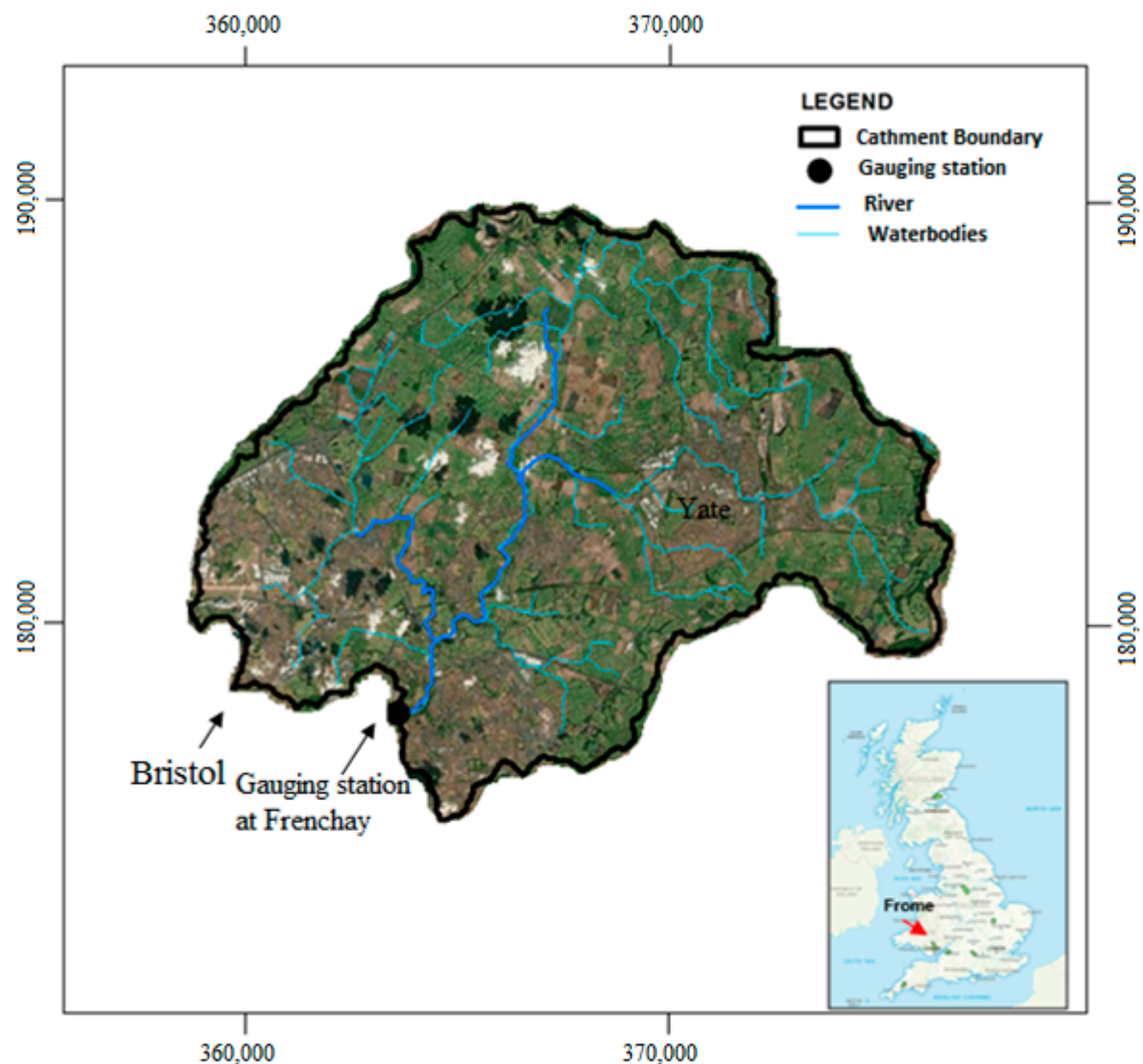


Figure 1. The River Frome, its catchment boundary and the location of the gauging station.

2.2. Data

For the modelling study, the catchment was divided into 195 grid squares, each of which has 1 km² area. The model was run on daily time step. The model input requires a number of climatic variables, including daily precipitation, daily temperature, daily wind speed, daily net radiation or daily total radiation and daily vapour pressure. Climate data were obtained from the Climate, Hydrology and Ecology research Support System (CHESS) that accounted for the impact of changes in elevation of climatic data [16,17]. The historic continuous climatic variables data were available from 1961, whereas the river-flow data were available from 1962 until 2012. The catchment boundary and gauging station location data were collected from the Centre for Ecology and Hydrology [18,19] and National River Flow Archive provided data for the daily river flow of the catchment [20]. The river and water bodies data were collected from the Centre for Ecology and Hydrology, Digital Rivers 50 km GB Web Map Service [21]. UK Land cover data were obtained from the Centre for Ecology and Hydrology (Land Cover Map 2007 (25 m raster, GB) Web Map Service [22]). The soil data were collected from data courtesy of Cranfield University, (1:250,000 Soilscales for England and Wales Web Map Service).

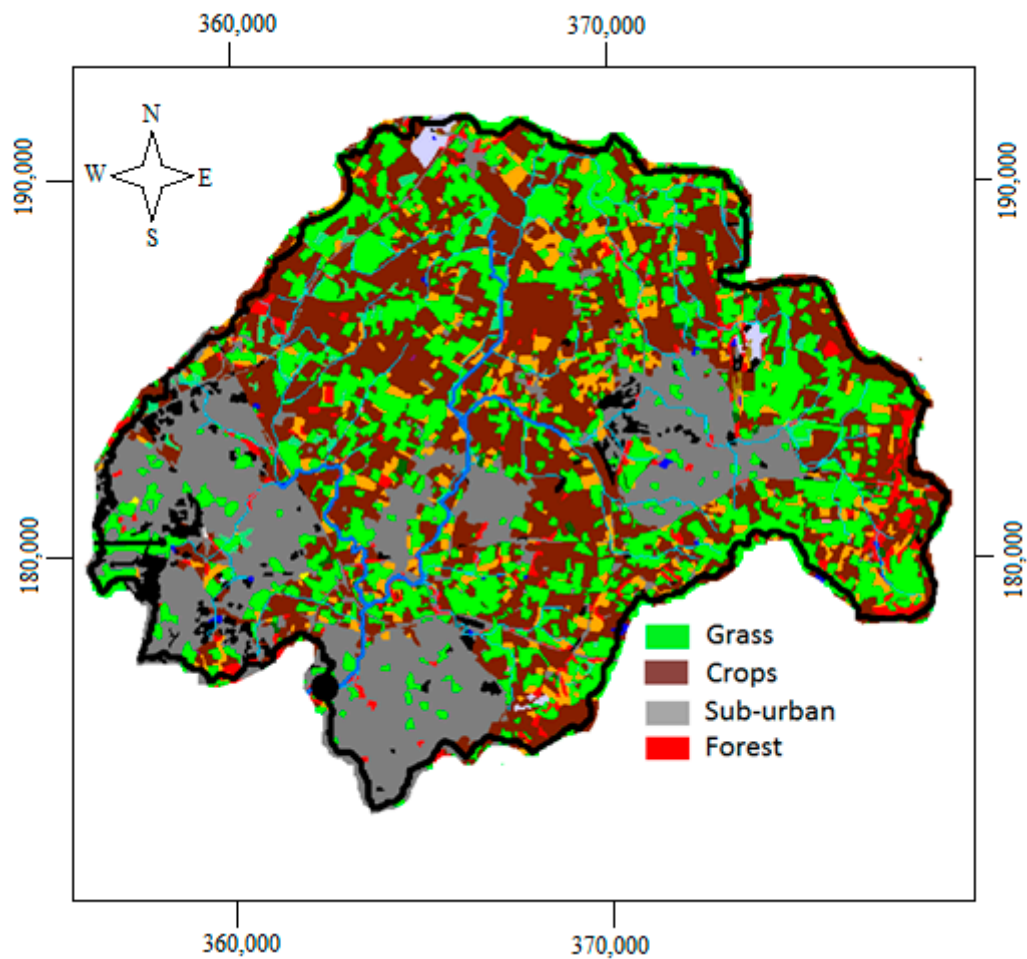


Figure 2. Key land use types in the Frome catchment.

2.3. Methodology

The schematic representation of the modelling work is shown in Figure 4, which shows the data sources used in the study. Both historic and future climatic variables data were used in the model to generate the streamflow, groundwater recharge, net rainfall, potential and actual evapotranspiration, Soil Moisture Deficit (SMD), Wetness Index (WI) of the root zone and water losses due to interception. All of these variables were used to calculate the drought risk for both the historic period and future climate change scenarios. Methodology about each drought index is discussed later.

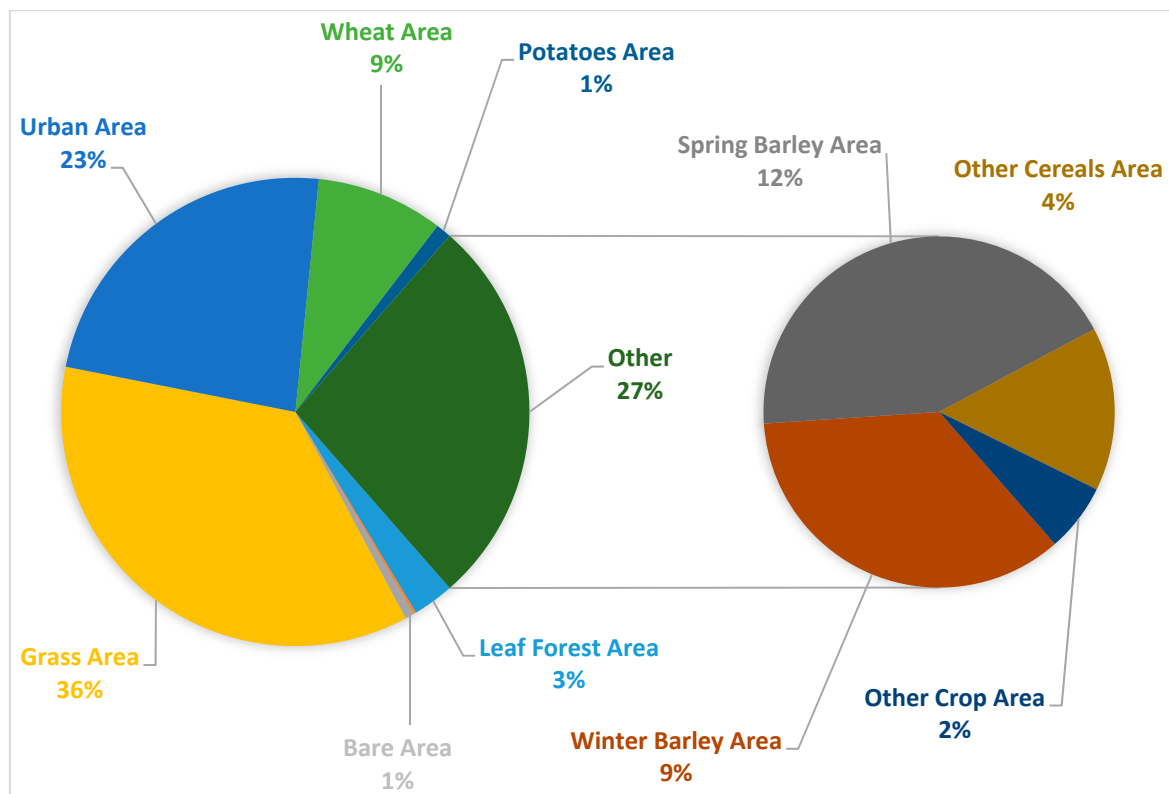


Figure 3. Detailed land use in the Frome catchment.

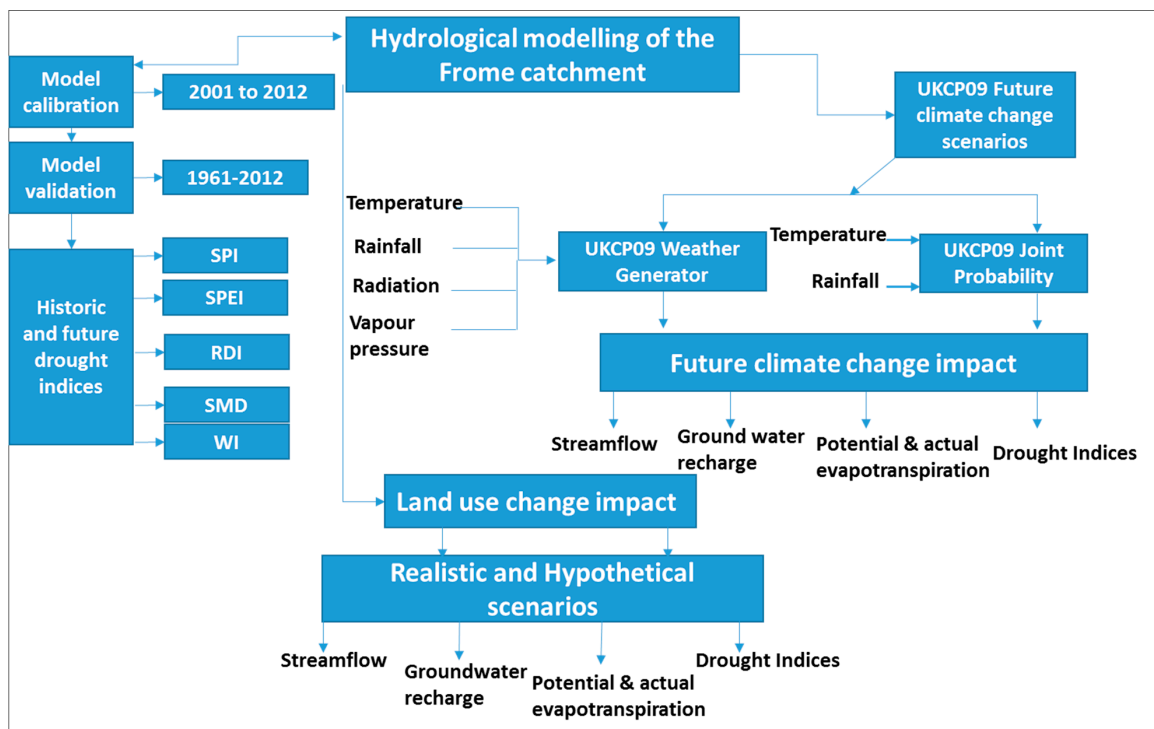


Figure 4. Frome catchment modelling work schematic representation.

The DiCaSM Model and Model Efficiency Measures

This study applied the DiCaSM (Distributed Catchment Scale Model) [23,24] hydrological model. The model is physically based and considers the commonly known hydrological processes such as rainfall interception, infiltration, evapotranspiration, surface runoff to streams, recharge to groundwater, water uptake by plants, soil moisture dynamics and streamflow. The model has been developed to estimate the catchment water balance components and to account for the impact of the changes in climate and land use on the catchment water resources, including streamflow and recharge to the groundwater. The model adopts a distributed approach with variable spatial scale (default in 1 km grid square) and requires daily input data of rainfall, temperature, wind speed, vapour pressure and radiation, and runs on a daily time step; however, if hourly rainfall data is available, the model can run with hourly time step. The model also addresses the heterogeneity of input parameters of soil and land cover within the grid square using three different algorithms [23]. The key model components are given in detail in Ragab and Bromley [23,24]. Briefly, they are the rainfall interception by grass, crops and trees, potential evapotranspiration of mixed vegetation, infiltration, recharge to the groundwater, surface runoff, stream flow, catchment water balance and root zone water balance. Further details about the model are given in [23,24].

In the DiCaSM model, the streamflow significantly depends on five key parameters: the percentage of surface runoff routed to stream, catchment storage/time lag coefficient, exponent function describing the peak flows, stream storage/time lag coefficient and the stream bed infiltration/leakage. At the start of the model calibration process, the model was run by changing all five key parameters using different time periods' data, and the best time period was selected for possible use for the model calibration. This was followed by the optimization process based on a simple iteration algorithm in which each of the five parameters were assigned a realistic range. Each range was divided into smaller steps, and the number of total iterations is the product of multiplication of the steps of the five key parameters. The number of iterations for each parameter was assigned according to the parameter sensitivity, i.e., a higher number of iterations were assigned to parameters which showed more sensitivity to the streamflow. The model calculates the Nash-Sutcliffe Efficiency (NSE) value for each iteration based on the least square of the difference between the simulated and observed streamflow values. The model optimisation process helps in finding a good set of parameters that produces a good model efficiency value.

The model calibration was carried out over 12-years, with the most recent data (2001–2012) and the validation period varying from a number of years to the entire available record. To determine the model efficiency/goodness of fit, the simulated and observed flow data were compared using a number of indices, including the NSE coefficient based on [25]. NSE is the most widely used coefficient to assess the performance of hydrological models [26]. An NSE coefficient of 100% indicates a perfect match.

$$NSE = 100 - \frac{\sum_{i=1}^n (O_i - S_i)^2}{\sum_{i=1}^n (O_i - \bar{O})^2} \quad (1)$$

where O_i and S_i refer to the observed and simulated flow data, respectively, and \bar{O} is the mean of the observed data. The calibration procedure consisted of adjusting the relevant parameters to achieve the best model fit with the latter assessed using the NSE values. In addition, the model performance was also evaluated using the coefficient of determination, R^2 as:

$$R^2 = \left\{ \frac{1}{N} \frac{\sum [(y_0 - \bar{y}_0) (\bar{y}_s - \bar{y}_0)]}{\sigma y_0 - \sigma y_s} \right\} \quad (2)$$

where y_0 is the observed value, y_s is the simulated value, N is the total number of observations, \bar{y}_0 is the average measured value, \bar{y}_s is the average simulated value, σy_0 is the observed data standard

deviation and σy_s is the simulated data standard deviation. The values of the R^2 index range from 0 to 1, with one indicating perfect fit.

2.4. Impact of Climate Change on Future Hydrological Variables

To study the impact of climate change on water supply systems, the UK Climate Change Scenarios (UKCP09) which provide projections for the changes in the amount and seasonal variation of precipitation, temperature and other climatic variables such as vapour pressure and sunshine hours, have been used. The DiCaSM model requires the net radiation data. UKCP09 weather generator only provides daily sunshine hours, and so therefore daily radiation data were calculated using the sunshine hours according to Allen et al. [27]. Although UKCP09 climate change projections are provided for seven overlapping time periods and for three greenhouse gas emission scenarios, low, medium and high relative to the baseline time period (1961–1990), this study selected all three greenhouse gas emission scenarios for three 30-year periods: 2020s (2010–2039), 2050s (2040–2069) and 2080s (2070–2099) [28]. The UKCP09 provides monthly, seasonal and annual probabilistic change factors at 25 km by 25 km grid square resolution for precipitation and temperature. UKCP09 also provides daily weather generator output data at a 5 km² resolution for other climate variables, such as vapour pressure and sunshine hours. For the initial exploratory analysis, simplified change factors were derived from UKCP09 joint probability central estimates. The joint probability plot was used to generate seasonal climatic change factors (% change in rainfall and change in \pm °C temperature) to apply as an input to the DiCaSM model. For the detailed weather generator simulations, 100 realisations of the daily time series data were generated in order to account for the uncertainty associated with the scenarios and alternative timing of events. A similar approach has been used by other researchers, including [29–31]. Table 1 shows the changes in precipitation and temperature under different climate change scenarios for three selected time periods: the 2020s, 2050s and 2080s, when selecting the joint probability plots of UKCP09. Table 1 shows the climate modelling central estimates of the joint probability plot (UKCP09) compared to the 1961–1990 baseline period. These probabilistic climate predictions are based on families of runs of the Met Office Hadley Centre climate models HadCM3, HadRM3 and HadSM3, combined with other climate models from different climate centres contributing to Intergovernmental Panel on Climate Change (IPCC AR4) and Coupled Model Intercomparison Project (CMIP3). The changes in global temperature are taken from three emissions scenarios: low (IPCC SRES: B1), medium (IPCC SRES: A1B) and high (IPCC SRES: A1F1), and each scenario provides estimates over seven 30-year overlapping time periods, where in this study three time periods (2020s, 2050s and 2080s) were selected (Table 1).

Based on historic data, the average annual rainfall for the Frome catchment is 792 mm and the average temperature is 9.7 °C for the baseline data. The seasonal temperature shows an increase with emission scenario and time, particularly in summer and autumn, whereas the precipitation is showing rainfall decreases in summer and increases in winter. The daily climate variables data generated using UKCP09 weather generator were bias corrected using the catchment observation data for the 1961–1990 period. This bias correction was needed as the predictions of UKCP09 were based on the whole UK baseline data. The bias correction was conducted before undertaking the modelling work. This study applied bias correction method using the quantile mapping “qmap” package in R statistical tool [32]. The main principle of quantile mapping method is to adjust the distribution of the climate model outputs so that it closely resembles the observed climatology [33].

Table 1. Probabilistic changes in temperature and precipitation for the Frome catchment under UKCP09 climate change scenarios under low, medium and high emission scenarios for the 2020s, 2050s and 2080s (30-years' time periods) using the Joint Probability data.

Climate Time		Low Emissions					Medium Emissions					High Emissions				
Variable	Period	Winter	Spring	Summer	Autumn	Annual	Winter	Spring	Summer	Autumn	Annual	Winter	Spring	Summer	Autumn	Annual
Change in Precipitation (%)	2020s	4.7	2.5	−6.7	4.23	1.18	5.7	0.97	−7.52	1.8	0.24	6.1	1	−8.16	1.61	0.14
	2050s	10.5	1.79	−9.5	2.17	1.24	17.24	0.03	−14	4.8	2.02	15.7	0.4	−20	5	0.27
	2080s	17.3	1.4	−15.17	3.82	1.84	22.1	1.2	−20	4.56	1.97	23	1.1	−28	5.67	0.44
Change in Temperature (°C)	2020s	1.1	1.18	1.61	1.62	1.38	1.27	1.2	1.72	1.6	1.45	1.3	1.2	1.5	1.65	1.41
	2050s	1.7	1.7	2.32	2.39	2.03	1.89	1.96	2.4	2.8	2.26	1.9	2.1	3	2.9	2.48
	2080s	2.1	2.1	3.08	2.89	2.54	2.6	2.7	3.6	3.61	3.13	3	3.4	4.5	4.52	3.86

2.5. Identification of Drought Indices

A number of drought indices are being used to identify the drought events and the most commonly used index is known as the Standardized Precipitation Index (SPI) [34]. The index represents the deviation of precipitation from the long-term average where the negative values indicate below average dry periods and positive values indicate above average precipitation wet periods. As precipitation is the key climatic variable on which soil moisture deficit, streamflow and groundwater recharge depend, the SPI helps in findings all types of droughts, from agricultural to the hydrological drought. The SPI could also easily be used to quantify the severity of both dry and wet events. Another drought index used in this study is the Reconnaissance Drought Index (RDI), which is based on Tsakiris et al. [35]. The RDI is calculated using the ratio of precipitation to potential evapotranspiration over a certain period. It is a good indicator for describing agricultural, hydrological and meteorological drought. The Reconnaissance Drought Index (RDI) was calculated as:

$$a_0^{(i)} = \frac{\sum_{j=1}^{12} P_{ij}}{\sum_{j=1}^{12} PET_{or} AE_{ij}} \quad (3)$$

$$RDI_n^i = \frac{a_0^{(i)}}{\bar{a}_0} - 1 \quad (4)$$

$$RDI_{st(k)}^i = \frac{y_k^{(i)} - \bar{y}_k}{\hat{\sigma} y_k} \quad (5)$$

where P_{ij} and PET_{ij} and AE_{ij} are the precipitation, potential evapotranspiration and actual evapotranspiration of the j th month of the i th hydrological year (starting from October), respectively, \bar{a}_0 is the arithmetic mean of the a_0 calculated for the number of years. In the above equation y_i is the $\ln(a_0^{(i)})$, \bar{y}_k is its arithmetic mean and $\hat{\sigma} y_k$ is its standard deviation. This drought index has been used in studies in different parts of the world, including Greece [36] and Iran [37]. This index is widely accepted and applied as it calculates the aggregated deficit between precipitation and the atmospheric evaporation demand. The index is directly linked to the climate conditions of a region and is comparable to the FAO Aridity Index [35]. An adjusted RDI was calculated using the net rainfall (gross rainfall minus rainfall interception losses by canopy cover) and actual evapotranspiration.

In order to accurately quantify the RDI, one could use actual values instead of potential values. Total rainfall does not represent the actual rainfall that is ready for infiltration and surface runoff as some of the total rainfall gets intercepted by land cover and evaporates back to the atmosphere, and in the case of trees, the intercepted amount is significant. Therefore, if the amount of rainfall intercepted by canopy is not considered, there would be an overestimate of the amount of rain available for infiltration and runoff, and subsequently an overestimate of the fluxes (stream flow, groundwater recharge, transpiration, bare soil evaporation, etc.). Potential evapotranspiration represents the atmospheric demand for water and reflects the potential ability of soil and plants to transport water from soil to the atmosphere. Plants can only transpire at potential level, and soil can only evaporate at potential level if soil moisture is at maximum holding capacity. During drought events, soil moisture falls well below maximum holding capacity, and neither the plant nor the soil can transport water to the atmosphere at potential level; therefore, it makes sense to use net rainfall and actual evapotranspiration (plant transpiration and bare soil evaporation) in calculating the RDI. If soil moisture is at maximum holding capacity, actual evapotranspiration will be equal to potential evapotranspiration. However, RDI is commonly used with gross rainfall and potential evapotranspiration because these two parameters are easily obtainable from weather stations while using net rainfall and actual evapotranspiration requires either processes based modelling and/or field measurements to quantify the intercepted water by canopies and the actual evaporation using measurements by for example Eddy Covariance or Scintillimeters or Lysimeters. One should bear in mind indices based on actual, not potential

input, will produce actual not potential values, and that is the reason for introducing the adjusted RDI especially for drought study under which the plants are subjected to water stress, reduced water uptake and reduced transpiration well below the potential level. The same for soil under drought, bare soil will not be able to evaporate at potential level as the soil moisture level drops below maximum water holding capacity. In drought conditions, it makes more sense to use the actual evapotranspiration.

Two other drought indices were considered: the soil moisture deficit (SMD) and wetness index (WI) of the root-zone. The SMD is the difference between current soil moisture and the maximum water holding capacity of the soil known as Field Capacity. The, WI is the scaled soil moisture: 1: soil water content at maximum value, 0: the soil water content at its minimum value. The WI accounts for the spatial variability of soil types, elevation and vegetation cover across the catchment.

Using a range of drought indices helps in identifying different types of droughts, i.e., the SPI index is relevant for meteorological drought, which is significantly based on rainfall deficiency, whereas hydrological drought is commonly associated with shortfall in runoff or groundwater recharge with WI as relevant index, and for the agricultural drought, where availability of the soil water is key for the crop growth, with SMD and RDI are relevant indicators for identifying the drought periods and a need for irrigation.

3. Results

3.1. Model Calibration/Validation for Streamflow

Results of the model calibration for the period 2001–2012 are shown in Figure 5, which illustrates that the model performance was very satisfactory during the model calibration period and the model responded well to rainfall events. The figure shows that the simulated values are mirror image to the observed values. During the model calibration stage model efficiency measured using the NSE efficiency was over 85% and the percentage error was less than 1%.

After the calibration, the model was validated over longer periods of up to ten years and then over the entire available record. An example of model validation during the 1970s (1971–1980) drought period showed that the model performed very well as the NSE efficiency was above 80%, and the percentage error between the observed and modelled flow was less than 5% (Table 2). This time period was selected to see the model performance during a long-term drought period, which significantly affected the soil characteristics and soil moisture deficit, and consequently affected streamflow and groundwater recharge. Considering the model efficiency over different climate conditions, the model showed an ability to estimate river flows. Results of the model comparison between the simulated and measured flow are shown in Table 2. The table shows the results of model prediction efficiency calculated in percentage as NSE or as R^2 values or percentage error.

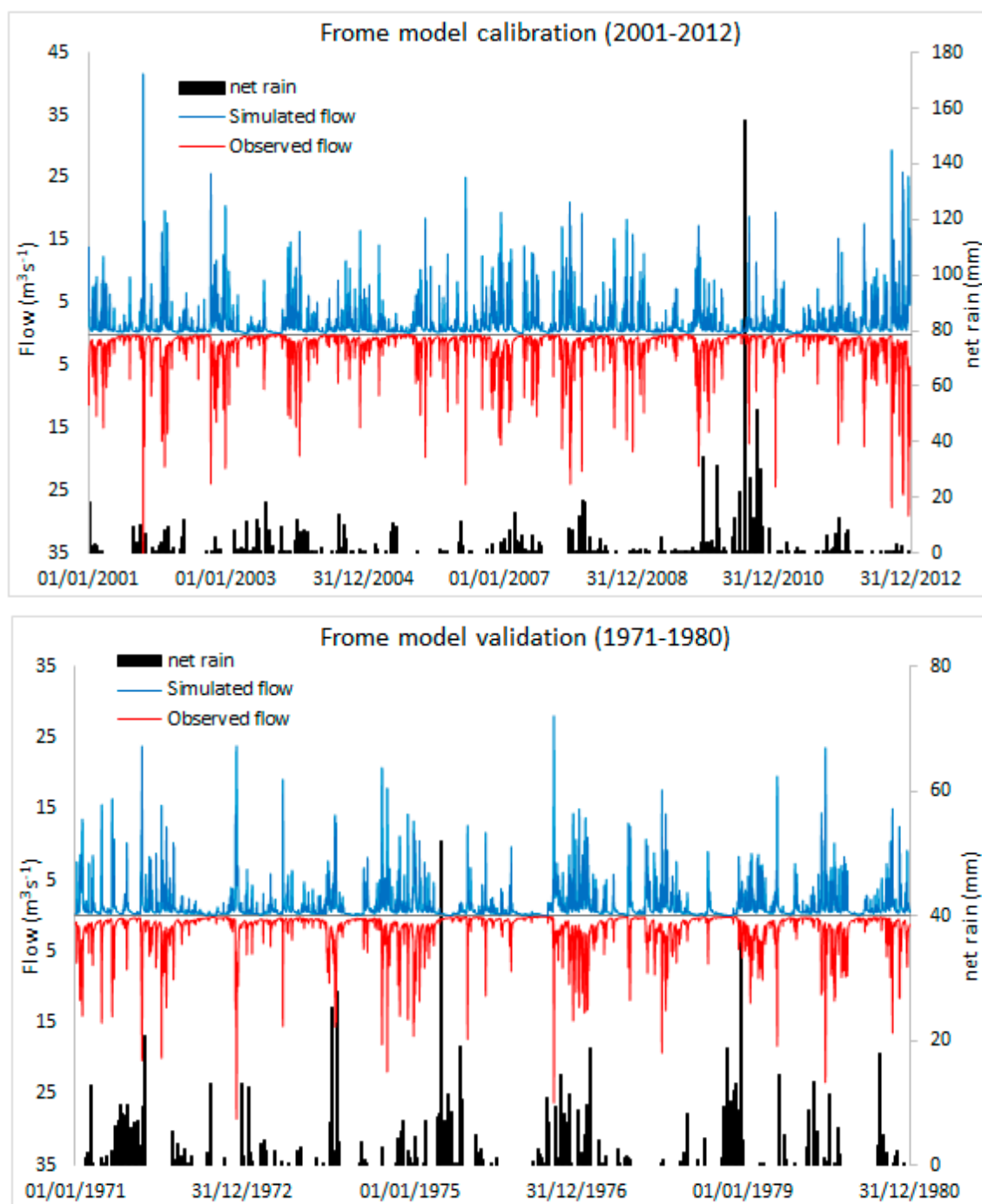


Figure 5. Model calibration of streamflow during the 2001–2012 and validation for the period 1971–1980.

In addition to the rainfall, another key climatic variable which affects the water balance, including surface runoff and streamflow, is the temperature and its impact on water losses by evapotranspiration. An example of the daily Frome evapotranspiration is shown in Figure 6, which illustrates the simulated actual evapotranspiration during the 1992–1994 period. The figure shows that actual evapotranspiration, as expected, is higher during the summer months (June, July, August) when rainfall was lower, and temperature was higher than in other seasons. The correlation between the observed and simulated flow of different time periods is shown in Figure 7. The figure shows the model capability to reasonably predict stream flows both during the model calibration and validation periods. The correlation between the observed and simulated flow shows that the model performed equally well during the extremely

dry and wet events. Model validation over 10-year sub-periods helped to find model performance during the drought i.e., the 1970s, and wet periods of the 1990s. The model results revealed a good agreement between the observed and simulated flows during both the dry and wet decades.

Table 2. Model performance during the calibration and validation stages of the Frome streamflow.

Time Period	NSE %	R^2	Modelled Flow $\text{m}^3 \text{s}^{-1}$	Observed Flow $\text{m}^3 \text{s}^{-1}$	% Error
2001–2012 *	85.5	0.86	1.79	1.78	0.94
1962–1970	81.7	0.83	1.69	1.71	−1.30
1971–1980	80.3	0.81	1.56	1.48	4.93
1981–1990	79.9	0.81	1.76	1.74	1.06
1991–2000	81.4	0.82	1.89	1.88	0.51
1962–2012	82.3	0.83	1.71	1.74	−2.25

* calibration period.

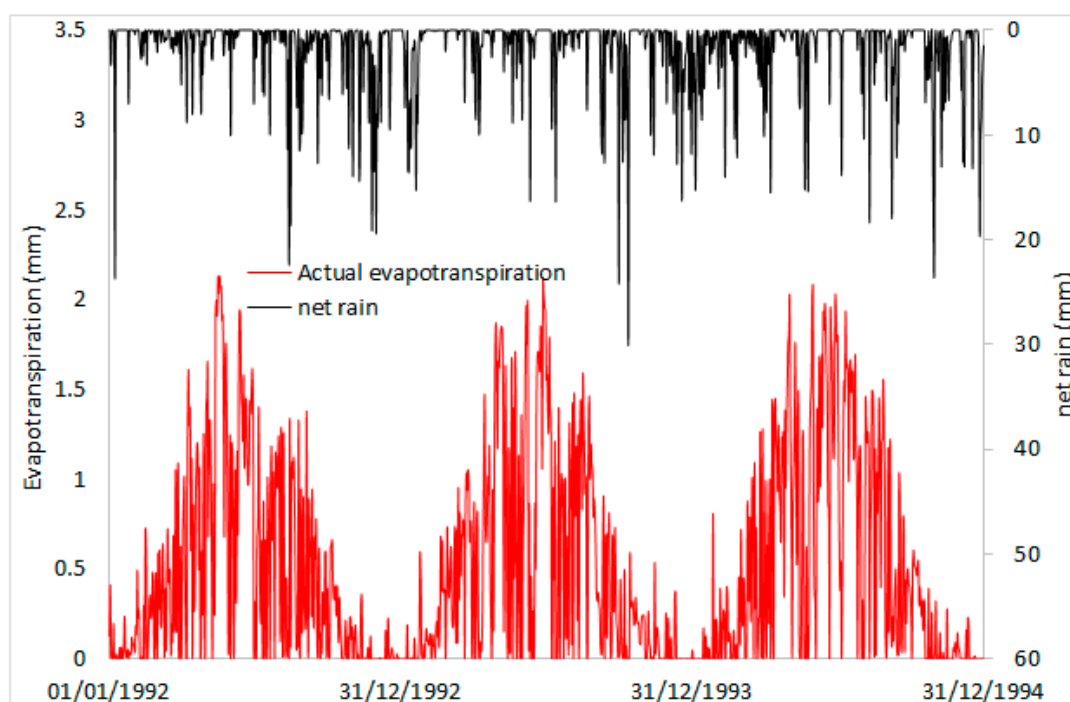


Figure 6. The actual evapotranspiration and net-rainfall for the Frome catchment during the drought period 1992–1994.

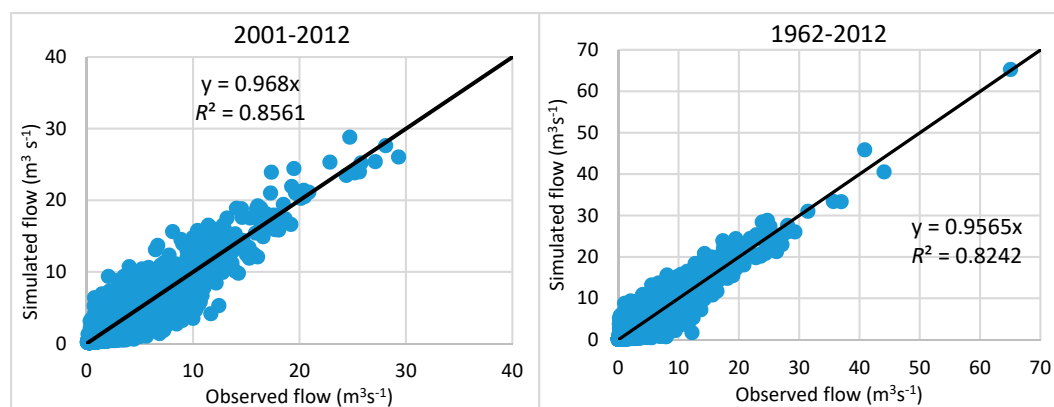


Figure 7. Cont.

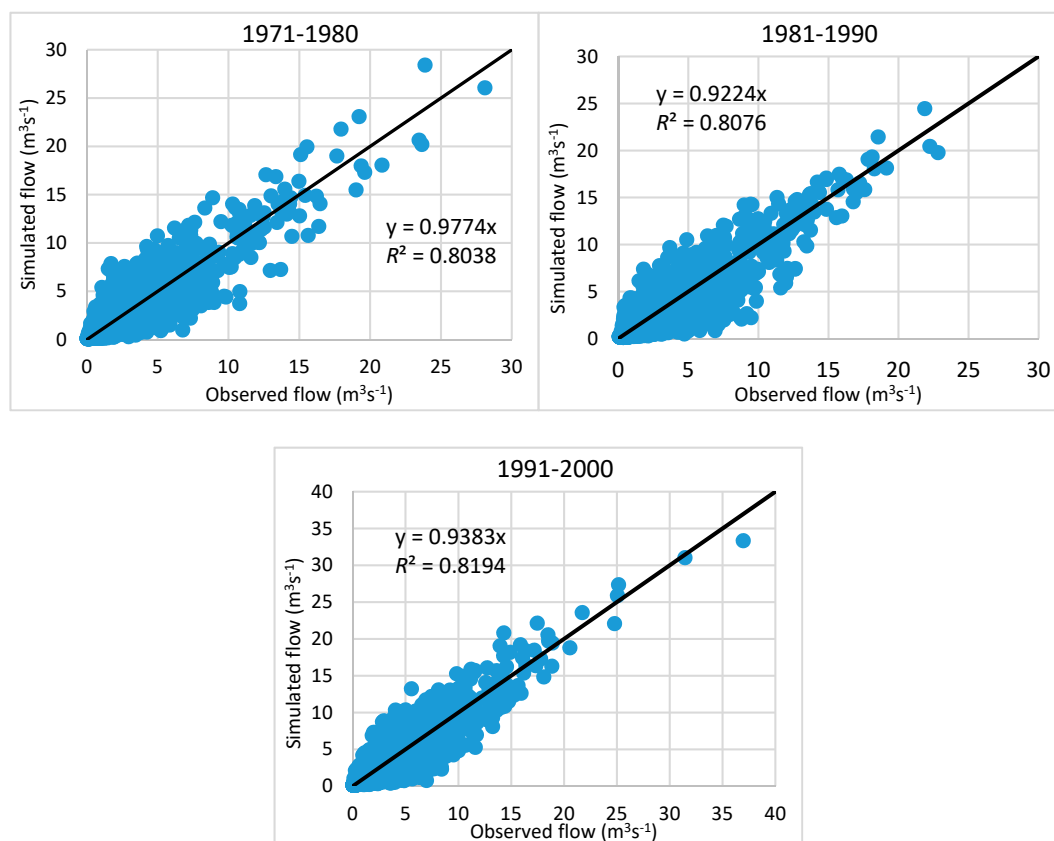


Figure 7. Relationship between the observed and simulated daily flow of the River Frome in Bristol.

3.2. Identification of Historic Droughts

3.2.1. The Standardized Precipitation Index (SPI)

The SPI is the most commonly used drought index and describes the deviation of the precipitation from the average precipitation. The SPI index scale values mean: above 2.0 extremely wet, 1.5–1.99 very wet, 1.0–1.49 moderately wet, -0.99 to 0.99 near normal, -1.0 to -1.49 moderately dry, -1.5 to -1.99 severely dry and -2.0 and less, extremely dry [34]. A number of studies including [38] in Cyprus, [39,40] in Greece used the SPI index, while [41] used the SPI index to manage the drought in transboundary watersheds between Iran and Iraq. The SPI index was calculated over six months which helps to identify any short drought event. This is well evident from the fact that the SPI index picked up all the drought events that took place in the Frome catchment between 1961 and 2012 (Figure 8).

The SPI index crossed over the extreme drought level during the most well-known 1970s drought which affected most parts of the UK and Europe. In addition, in the Frome catchment, drought events also took place in the earlier part of the 1960s, which could be considered regional drought episodes. Phillips and McGregor [13] classified the early 1960s drought as a class-1 drought. The streamflow and groundwater recharge also depend on other climatic variables like temperature and radiation as they affect the water losses by evapotranspiration, but precipitation variations have an immediate impact on the streamflow and groundwater recharge. Therefore, SPI index could also be used as a good indicator for meteorological drought. Over the 52-year study period, the SPI index elucidated all the main dry events, like those that occurred in the 1970s. The SPI index also helps in identifying smaller magnitude drought events or drier periods which took place in the late 1960s, early 1990s, 2003–2004, and in 2009 and 2010. The magnitude of the severity of drought was considered severe in the early 1960s, in the mid-1970s, in 1976 and in 1995 where the SPI index crossed -3 , considered an extreme drought.

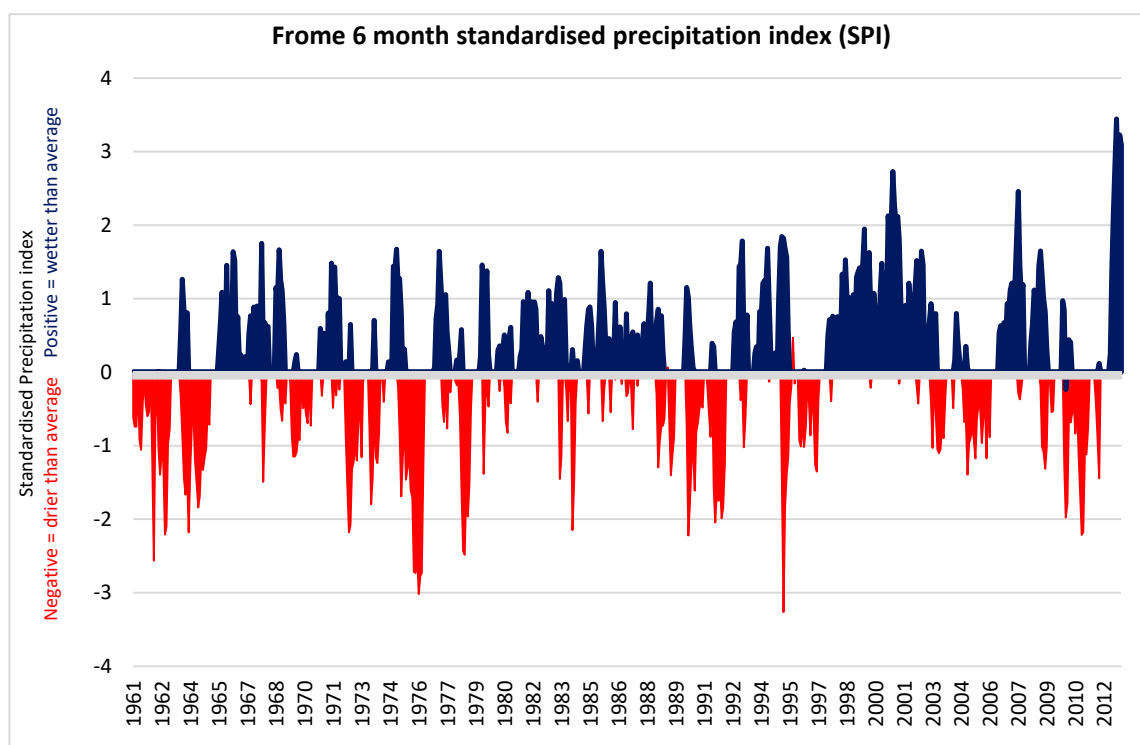


Figure 8. Six months standardized precipitation index (SPI) of the Frome catchment from 1961 to 2012.

3.2.2. Reconnaissance Drought Index (RDI)

The other drought index that was considered in the study was the Reconnaissance Drought Index (RDI) which uses the ratio of total rainfall to total evapotranspiration of a period to represent the hydrological system input/output balance. Should the output (losses) exceed the input, drier conditions and eventually drought would occur. In this study, an attempt was also made to use the actual evapotranspiration and net rainfall to calculate the Adjusted RDI. The RDI index also picked up all the drought events which were observed by the SPI drought index. However, the advantage of applying RDI drought index is that it does not rely only on one factor, i.e., precipitation as it calculates the index using the rainfall relationship to the evapotranspiration and therefore implicitly incorporates the important influence of meteorological variables, such as temperature. Figure 9 shows the comparison between the RDI, and the Adjusted RDI. The Adjusted RDI showed slightly different severity levels, as its input in terms of rainfall (net rain) is less than the input to RDI (total rainfall) and output is also less (actual evapotranspiration) than the RDI (potential evapotranspiration) especially during extreme drought events. Figures 8 and 9 show a strong trend resemblance between the RDI and the SPI. Figures 8 and 9 show that extreme drought conditions were observed in 1976 as SPI and RDI both reached a low value of -2 under both types of RDI. Drier than average spells (SPI or RDI less than -1) were also observed in 1964, 1989, 1996, 2005, 2009 and 2011.

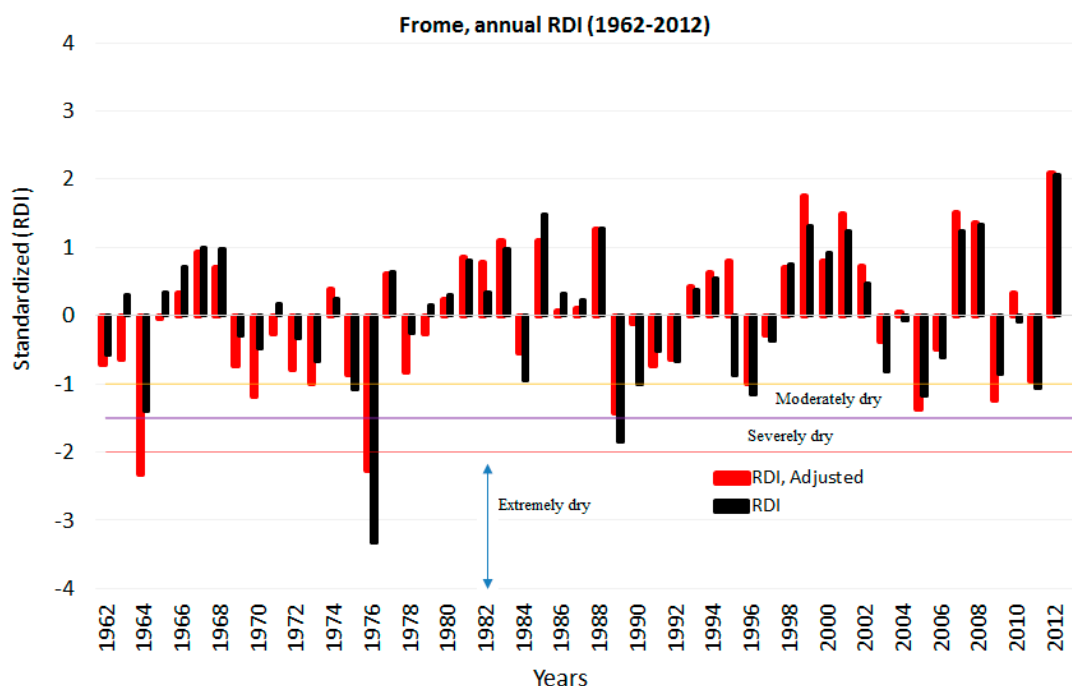


Figure 9. Historic annual reconnaissance drought index (RDI) of the Frome catchment from 1961 to 2012.

3.2.3. Soil Moisture Deficit, SMD and Soil Wetness Index, WI as Drought Indicators

The other drought indices which are more relevant to study the agricultural drought are soil moisture deficit, SMD and the wetness index (WI) of the root-zone. The WI represents how relatively wet or dry the catchment is over a period. When the WI value is 1, the catchment is at its maximum soil moisture and when WI is zero, the catchment is at its minimum soil moisture content (Figure 10).

The SMD represents the deviation of actual soil moisture from the soil moisture at field capacity. Here, zero means the catchment's soil moisture is at field capacity level. The deviation gets larger when the soil moisture starts to fall below the field capacity, especially during summer and during drought periods. Examples of both indices are shown in Figure 10 which clearly shows the soil moisture indicators WI and SMD during the dry summer months, especially, the extreme drought in 1975 and 1976, and the recovery in 1977. In the dry summer months of 1976, soil moisture deficit reached over 80 mm and, in the summer of 1976, the soil moisture deficit reached 116 mm. The figure also shows the severity of dry spells as a result of the continuation of the dry seasons including the 1975–1976 winter months as the SMD could not drop down to zero, whereas in the 1977 winter months above average winter rainfall brought SMD back to zero. It can also be seen that the WI dropped down below the winter value of 1.0 to 0.1 during the extreme drought of the summer of 1976 while the SMD mirrored the trend of WI.

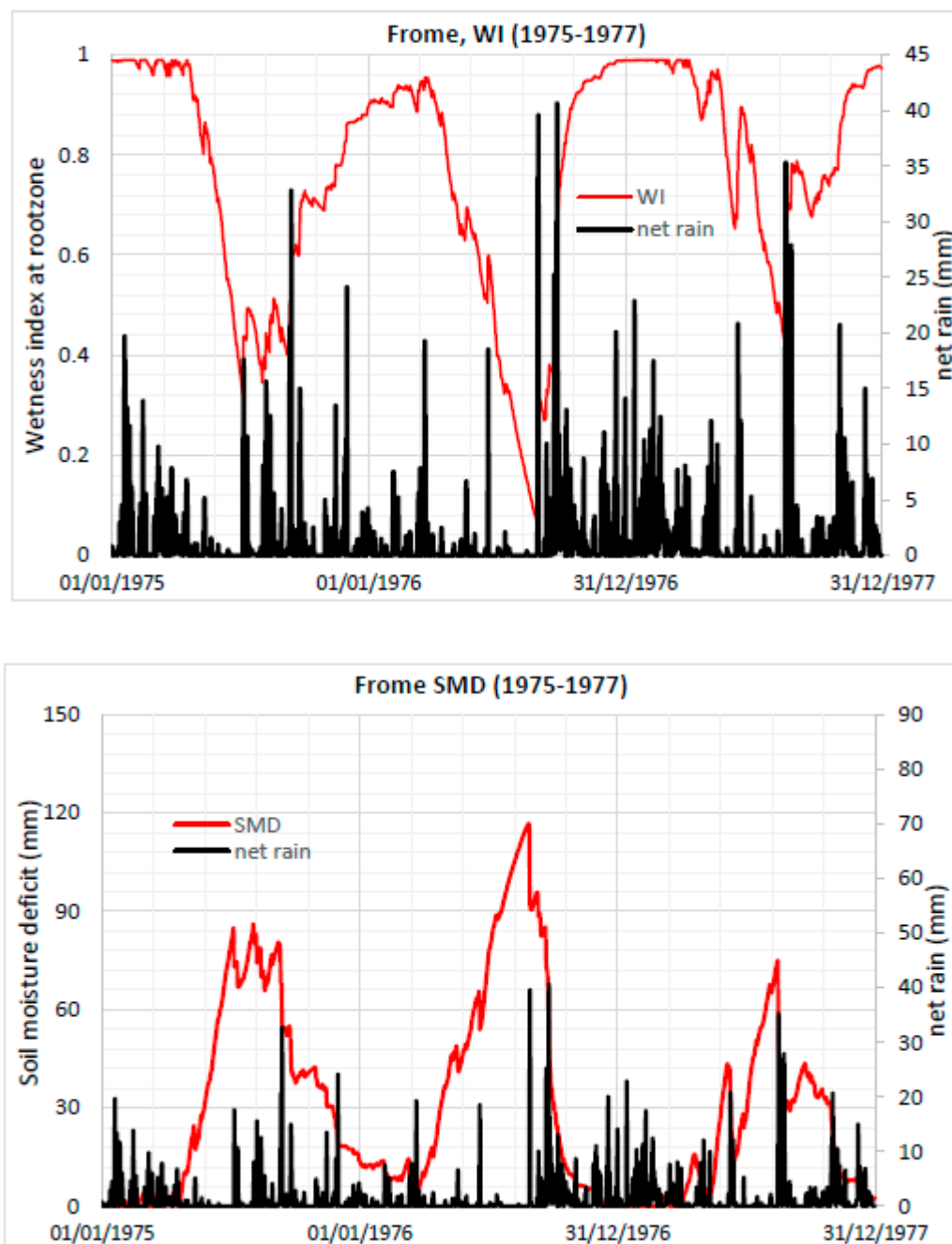


Figure 10. Wetness Index (**top**) and soil moisture deficit (**bottom**) of the root-zone for the Frome catchment during 1975–1977 drought period.

3.3. Future Hydrological Changes and the Drought Indices

3.3.1. Changes in Streamflow

As described under Section 2.4, under all future emission scenarios of the UKCP09, the expectation is a strong likelihood of lower summer rainfall and higher summer temperatures that will be felt all over the UK. All three greenhouse gas emission scenarios for three 30-year periods: 2020s (2010–2039), 2050s (2040–2069) and 2080s (2070–2099) were selected and Joint Probability data and the Weather Generator data were used as an input to the DiCaSM model. In the case of Weather generator data, three periods, three emission levels and 100 realisations daily input files per period per emission were generated in order to account for the uncertainty associated with the scenarios and alternative timing

of events. In total, 900 files were used as input. Results of the 100 files of each emission and period were averaged to produce a single daily value representing the variations among the 100 files. Average monthly, average seasonal and average annual values were produced from the average daily values. The results were compared with the baseline data of 1961–1990. Percent changes relative to base line data (1961–1990) were calculated and presented hereafter.

The streamflow projections under both the simplified change factors provided by the joint probability and the weather generator data suggest that the streamflow is likely to be reduced under all emission scenarios, except during winter when the streamflow is likely to increase by 9% in the 2050s and 2080s under medium and high emission scenarios, the increase under low emission in the 2080s would only slightly below 9% (Figure 11). A lower increase of 4 to 5% is projected for the 2020s under medium and high emissions; during the 2020s, the increase would be approximately 1%. During spring, the river flow is likely to decrease and the highest decrease in projected for the 2080s under high emission scenarios when river-flow could decrease more than 10% in comparison with the baseline period. Overall, an annual decrease in streamflow was observed under medium and high emission scenarios in the 2080s in comparison with the baseline period (1961–1990).

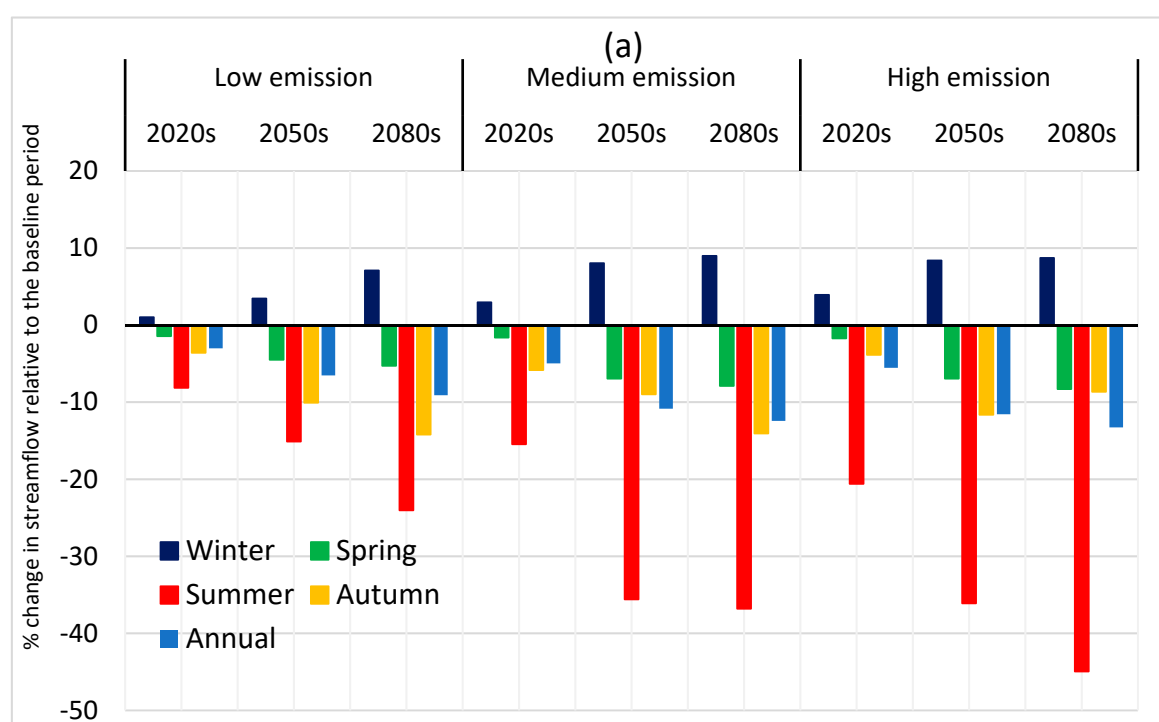


Figure 11. Cont.

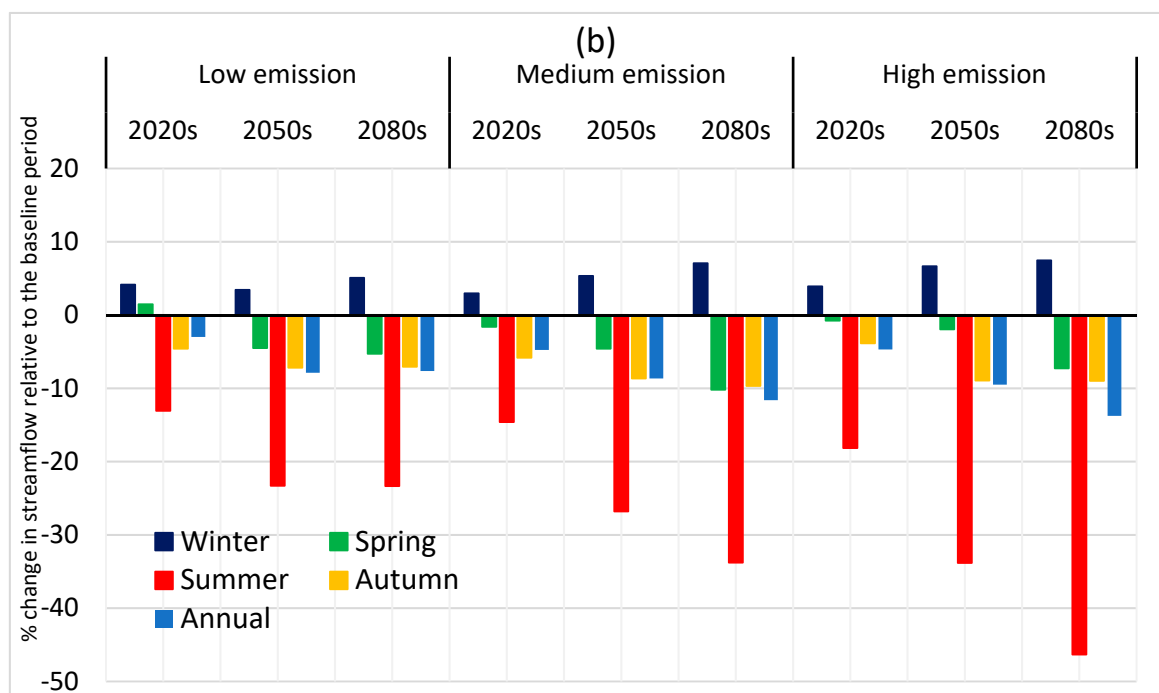


Figure 11. Changes in streamflow using joint probability (a) and weather generator (b) data of the UKCP09 different climate change scenarios.

Under all emission scenarios, the summer streamflow is likely to decrease by 8.13% to 20.58% in the 2020s, by 25% to 36% in the 2050s and by up-to 45% in the 2080s under high emission scenarios using the joint probability and the weather generator data. UKCP09 weather generator also projects a decrease in streamflow in the summer season for all time periods and the highest decrease is projected for the 2080s when streamflow could decrease by 46.3% under high emission scenarios. Up to a 37% decrease is projected under medium emission scenarios in the 2080s. No significant decrease in streamflow is projected under low emission scenarios for all seasons, including summer, when using the UKCP09 weather generator and joint probability of the UKC09. Under low emission scenarios, the streamflow could decrease by 8% in the 2020s, and by up to 25% in the 2080s in summer season both under weather generator and the joint probability. This decrease in streamflow is likely to continue in the autumn season when flow could decrease by up to 14% and 10% when applying the joint probability and weather generator data of the UKCP09, respectively, under medium and high emission scenarios for the 2050s and 2080s. This decrease, particularly during the summer, could lead to very low stream flows, possibly leading to high risk of inadequate domestic, industrial and agricultural water supply. The latter is more important for the Frome catchment as river water abstraction is very significant during the summer and first part of the autumn due to agricultural activities.

3.3.2. Changes in Groundwater Recharge

Climate change could significantly affect the groundwater recharge in the catchment. Despite the fact that the climate change models project an increase in winter months under all emission scenarios, the groundwater recharge is shown to vary according to the season. For example, under all emission scenarios, the groundwater recharge is likely to increase in winter from 4.5 to 8.5% under all emission scenarios in three projected time periods: the 2020s, 2050s and 2080s (Figure 12). Although climate models suggest a significant increase in winter precipitation, this increase would be counterbalanced by the higher water losses due to the increased evapotranspiration resulting in a slight change in groundwater recharge in comparison to the change in precipitation.

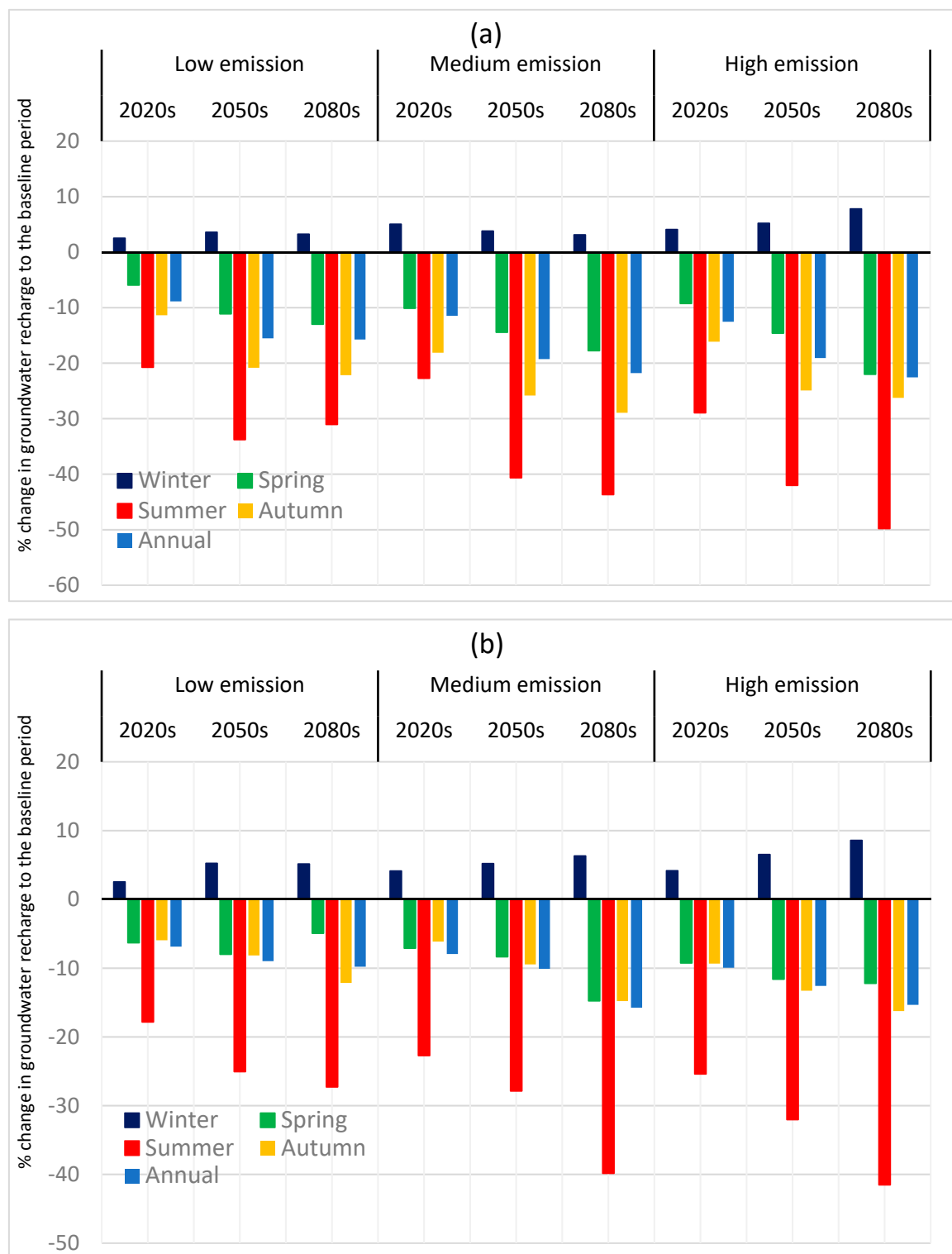


Figure 12. Changes in groundwater recharge using joint probability (a) and weather generator (b) data of the UKCP09 different climate change scenarios.

During the spring season, under all emission scenarios, a likely decrease in groundwater recharge is projected for all selected time periods. This decrease is likely to continue during the summer months due to the expected low summer precipitation and increasing temperature, which could lead to a decrease in groundwater recharge by up to 50% under high emission scenarios of the 2080s when

using joint probability data of the UKCP09 data, albeit the percentage change in groundwater recharge was not that high when using the UKCP09 weather generator data. Such a significant decrease in groundwater recharge is the result of increased soil moisture deficit. Herrera-Pantoja and Hiscock [42] reported that the drier summers could lead to increased soil moisture deficit extending into the autumn and could shorten the winter recharge season. Overall, an annual decrease in groundwater recharge was observed under all emission scenarios, this decrease was slightly higher under medium and high emission scenarios in the 2080s in comparison to the baseline period. This decrease in winter groundwater recharge could be balanced by the increased winter precipitation as projected under all emission scenarios, as shown in Table 1. The future increase in winter precipitation is expected to come as extreme events and over a short period of time, as reported by Alexander et al. [43], and would result in reduced recharge. The results, shown in Figure 11, show that under all emission scenarios, the groundwater recharge is likely to decrease for all future time periods in spring, summer and autumn seasons. An increase in groundwater recharge during winter months is projected in the 2050s and 2080s; however, the increase is not that significant.

3.3.3. Drought Indices

To observe the impacts of climate change, drought indices including soil moisture deficit and wetness index at root-zone, and the reconnaissance drought index were applied in this study.

Future SMD, WI and Actual Evapotranspiration

The use of the daily projected data of the weather generator with the DiCaSM model for the future time periods suggested a possible increase in SMD, and an increase in actual evapotranspiration. The highest increase in soil moisture deficit was 160% under high emission scenarios during the 2080s (Figure 13). This is due to the decrease in precipitation and increase in temperature that resulted in higher evapotranspiration. Under the high emission scenario, the results of the time period of the 2080s showed an increase of around 130% in evapotranspiration.

This finding of the study is consistent with other studies, i.e., Charlton and Arnell [44] who studied six catchments across the UK and found increasing trends in evapotranspiration under climate change projections. This is well supported by Gosling [45] who suggested that the decreasing trend in streamflow of the studied catchments intensified over time due to the increased potential evaporation that outweighs the increasing trend of precipitation. Kay et al. [46] also reported an increase in future evapotranspiration in different parts of the UK, including the South-West, and found the highest increase in South-East England. Chun et al. [47] also reported that the southern parts of the UK will be more sensitive to the changes in evapotranspiration as compared to the north of the country. As expected, the biggest change in the actual evapotranspiration and soil moisture deficit was observed under high emission scenarios which significantly affect both the surface and groundwater resource availability. This is likely to be the result of an increase in temperature associated with lower precipitation. The projected increase in winter rainfall could be counterbalanced by the water losses due to both the high evapotranspiration and soil moisture deficit.

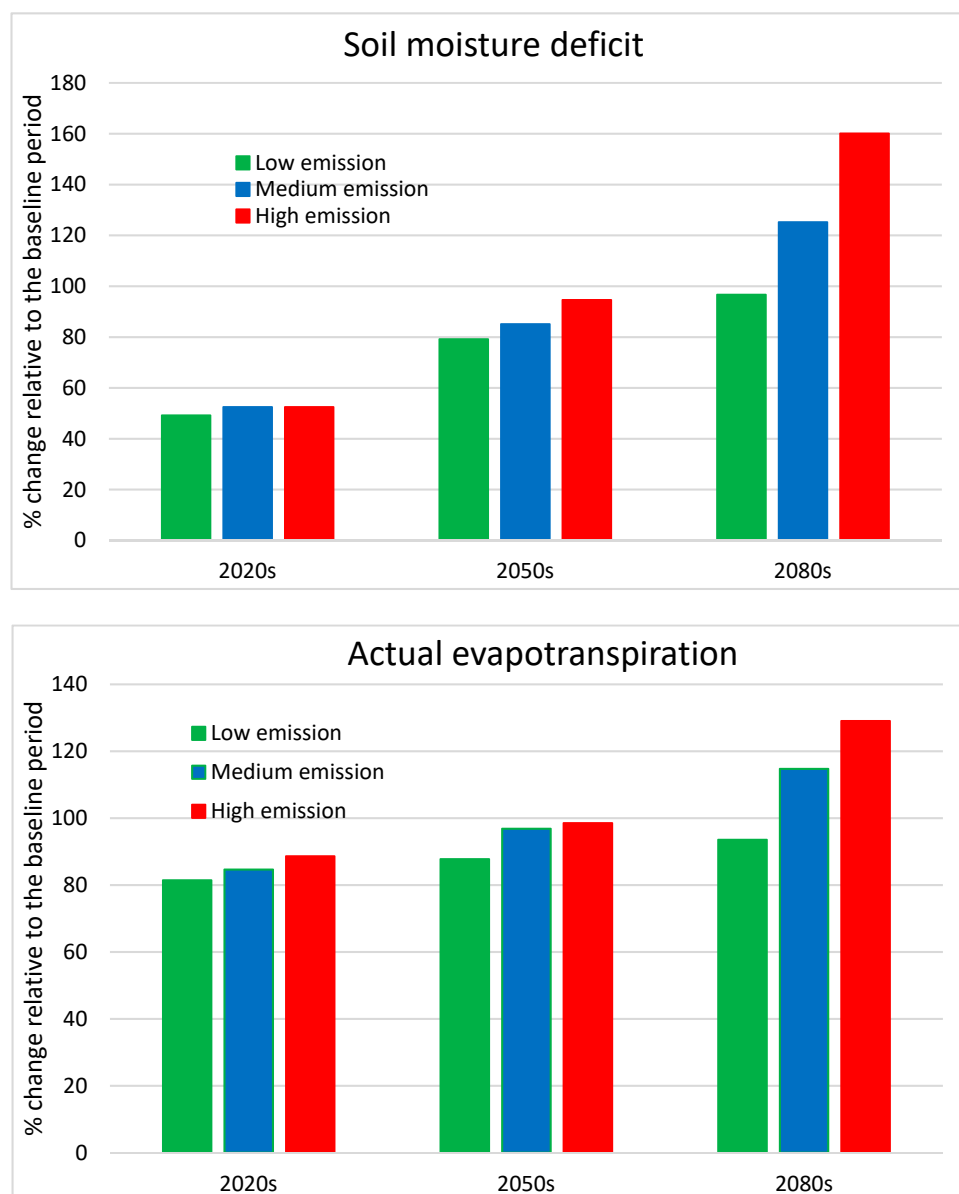


Figure 13. Soil moisture deficit (**top**) and actual evapotranspiration (**bottom**) projected under different climate change scenarios using UKCP09 weather generator data.

Future Reconnaissance Drought Index (RDI)

The RDI was calculated from the net rainfall and potential evapotranspiration of the selected time periods: 2020s, 2050s and 2080s for three emission scenarios. Like SPI index, the standardized reconnaissance drought RDI index scale values mean: above 2.0 extremely wet, 1.5–1.99 very wet, 1.0–1.49 moderately wet, −0.99 to 0.99 near normal, −1.0 to −1.49 moderately dry, −1.5 to −1.99 severely dry and −2.0 and less extremely dry [48]. Under low emission scenarios, the moderate drought events tripled in the 2050s and 2080s in comparison to the baseline period. This is possibly due to the mild and wet winters and drier and warmer summers, as shown in the Table 1. As projected for the low emission scenarios, a slight change in precipitation and temperature have led to drought severity level close to normal which is reflected in the higher number of moderate drought events (Figure 14). Under medium emission scenarios, the annual drought is considered severe as compared to the baseline period (1961–1990) and low emission scenarios. Under medium emission scenarios, the extreme drought events doubled in the later part of the century, in addition, more severe drought events were

also projected in the 2050s and 2080s when using the weather generator data. This is due to the drier and warmer spring, summer and autumn seasons, leading to higher water losses by evapotranspiration combined with below average rainfall, both could result in extreme and severe drought events. The analysis under medium emission scenarios reveals that the severity of the drought will become more significant in the later part of the century.

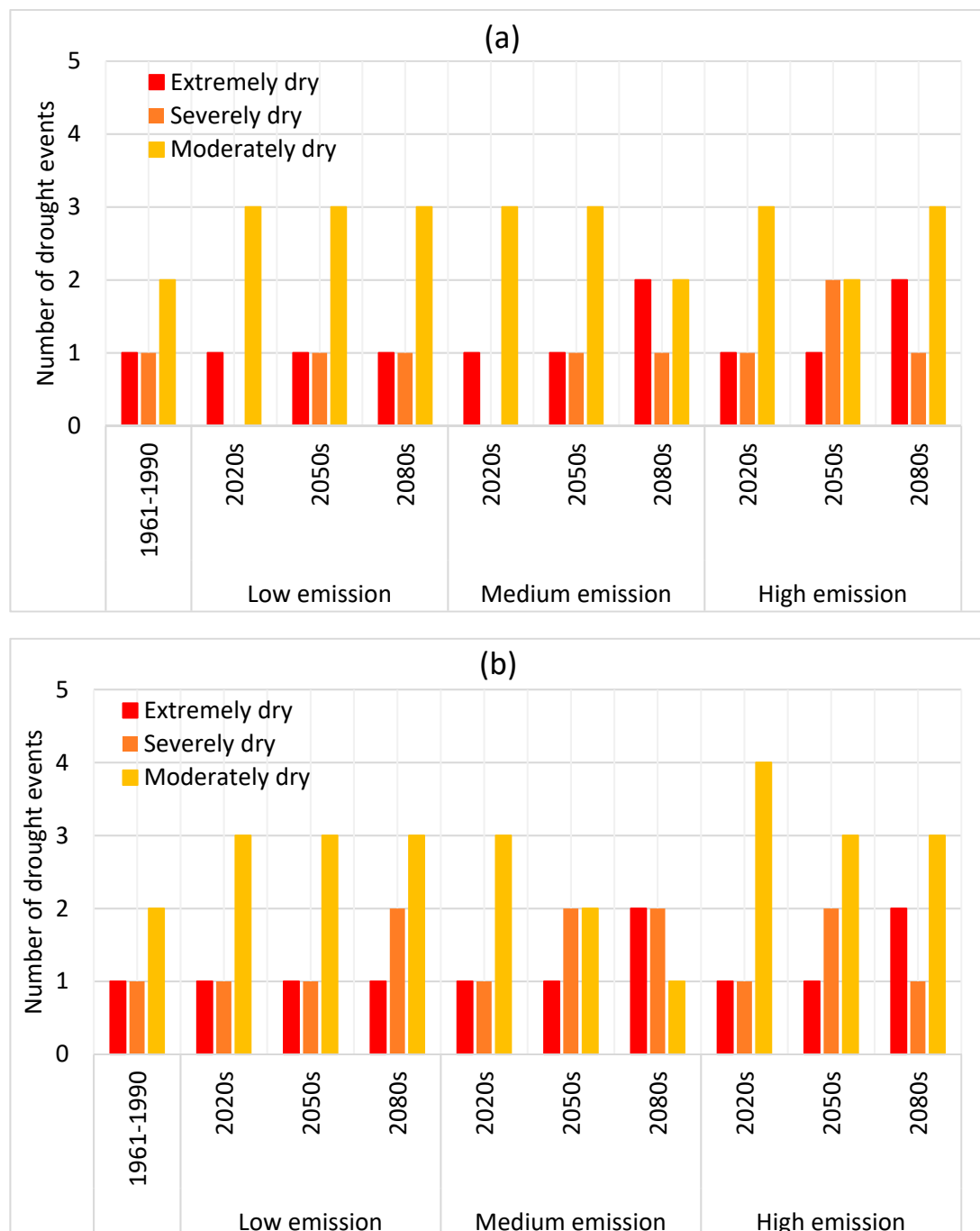


Figure 14. Drought event severity observed in the Frome catchment under low, medium and high emission scenarios for the 2020s, 2050s and 2080s, Figure (a) shows the drought severity using joint probability data and (b) when using the weather generator data.

Under high emission scenarios, for the three selected time periods, the severity of the drought events increased with time. In the 2020s, there was no significant change in the number of extreme and

severe drought events, but the number of moderate drought events almost doubled in comparison to the baseline period. However, in later part of the century, more extreme and severe events almost doubled due to the projected drier and warmer climatic conditions in the summer and autumn seasons using both the joint probability and weather generator data of the UKCP09.

3.4. Impacts of Land Use Changes on the Hydrological Variables

To study the impact of land use type, some realistic (plausible) and hypothetical land use scenarios were created as vegetation type significantly affects the proportion of the interception and the transpiration amount. Therefore, the temporal dynamics of the plant cover have a strong impact on initiation of the runoff and consequently the streamflow and groundwater recharge. Table 3 shows the analysis of the selected land use scenarios. The impact of the land use change on hydrological variables varies with the season, especially during the spring and summer season when crops take up more water and loose more water by the evapotranspiration which leads to increased soil moisture deficit and decrease in streamflow and groundwater recharge. When the highest rainfall is expected in spring season, the ground cover and land use type play a significant role in runoff generation, streamflow and groundwater recharge.

The possible and hypothetical land use changes considered showed a varying impact on the hydrological variables, the river flow and groundwater recharge. (Table 3). The table shows 6 scenarios:

1. If the grass area replaced by barley: river flow would increase by 14% in autumn and by less than 7% in all other seasons. Groundwater recharge would also increase by 13% in winter and by less than 7% in all other seasons.
2. If grass area replaced by oil seed rape: river flow would decrease of 21% in summer, 15% in spring and 6% in winter but a small increase of 3% in autumn is projected. A possible decrease in groundwater recharge by 21% in summer, 12% in spring, 5% in winter but possible small increase less than 4% in autumn are projected.
3. If 50% winter barley replaced by oil seed rape: reduction in streamflow around 7% in winter, spring and autumn and a small reduction less than 2% in summer are projected. Also, a decrease in groundwater recharge by 13% in summer, by less than 7% in winter and spring and by 1% in autumn are projected.
4. If 100% winter barley replaced by oil seed rape: A decrease in streamflow by around 14% in winter, spring and autumn but small decrease of less than 4% in summer are projected. Groundwater recharge is also expected to decrease between 9% to 23% during winter, spring, summer and by less than 2% in autumn.
5. If 40% increase in urban area replacing grass: an increase in streamflow between 11% to 19% in winter, spring and summer and around 9% in autumn are projected. Ground water is likely to decrease between 2% to 8%
6. If all crops replaced by broad leaved forest: A decrease in streamflow between 8% and 16% in winter, spring and summer and less than 5% in autumn are projected. The groundwater recharge is likely to decrease between 14% and 21% in spring and summer and by less than 1% in winter and 6% in autumn.

Generally, the results indicate that increasing urban areas would enhance surface runoff to streams. Also, replacing grass with winter barley would enhance streamflow and groundwater recharge. On contrary, replacing grass or barley by oil seed rape would reduce both streamflow and groundwater recharge. Also, if Broad Leaf Forest replaced the arable land, streamflow and groundwater recharge are expected to decrease.

Table 3. Impact of land use changes in the Frome catchment on selected hydrological variables.

Hydrological Variable	Seasons	Change in Land-Use Type					
		100% Grass Area Replaced by Barley	Grass Area Replaced by Oil Seed Rape	50% Winter Barley Replaced by Oil Seed Rape	100% Winter Barley Replaced by Oil Seed Rape	Grass Area Replaced by 40% Urban Expansion	All Crops Replaced as Broadleaved Forest
River flow	Winter	5.68	−6.47	−8.21	−14.49	10.55	−7.96
	Spring	6.91	−15.38	−6.72	−11.87	14.92	−10.59
	Summer	5.38	−20.85	−1.88	−3.55	18.93	−16.22
	Autumn	14.01	3.21	−7.14	−15.66	8.71	−4.79
Groundwater GW recharge	Winter	12.86	−4.90	−7.6	−13.94	−1.92	−0.65
	Spring	2.38	−11.92	−5.88	−8.82	−4.58	−14.36
	Summer	4.94	−20.64	−12.51	−22.81	−7.49	−20.92
	Autumn	7.07	3.63	−1.11	−1.81	−2.13	−5.89

The expansion of the broadleaf trees that have large canopies and deeper roots tend to take up a large amount of water from the root zone creating larger soil moisture deficit that results in a reduction in surface runoff generation and groundwater recharge. Oil seed rape to some extent has a deeper rooting system than grass and transpires more water leading to higher soil moisture deficit. Urban expansion could result in increased streamflow (likely to increase in flood risk). Overall, the effect of the land use changes on the hydrological variables was much less than the effect of climate change. However, considering the possible changes in climatic variables and extreme events in the future, sustainable land use practices could potentially be used to mitigate the impact of climate change on the catchment's water supplies.

4. Discussion

4.1. The Drought Indices

This study analysed the impact of climate change on the possible occurrence of drought events and the changes in streamflow and groundwater recharge of the Frome catchment. Several drought indices were used in the study and were able to identify all the historic droughts events, i.e., in the 1970s, 1980s and 1990s. As the reconnaissance drought index, calculated from the actual evapotranspiration and the net rainfall, showed slightly better results than the SPI, SMD and WI, the RDI was used as an indicator to identify future drought events. The standardized precipitation index, SPI, indicated the significant negative deviation from the average precipitation in the 1970s. This was well supported by the other drought indices like the RDI, soil moisture deficit, SMD and the WI of the root-zone (as shown for the period 1975–1977 in Figure 9).

Application of a wider range of drought indices could be used to identify different types of drought. For example, in agriculture, when SMD reaches a critical level, crops will require irrigation, particularly during the summer, which could affect the water supplies and the crop yield due to low water availability during the dry months. The WI of the root zone, if close to 1, would indicate a wet catchment with a possible runoff generation during the next rainfall event. It is a help to reservoir managers to know the WI in real time. RDI would be helpful for short and long-term planning by water authorities and water companies. The effect of low rainfall and high temperature could be expressed by the RDI drought index that was able to show more severity in the latter half of the century (Figure 14).

4.2. Climate Change Impact on Water Resources

The future climate change scenarios suggested a decrease in groundwater recharge which could decrease by more than 40% by the end of the century. Not only the groundwater recharge but also the streamflow is likely to decrease by 40% to 50% when using the weather generator and the joint probability data. Considering the possibility of such droughts in the future, the agriculture and irrigation practices need to be adapted for the future as reduced water supply could be problematic for the irrigation in summer. Considering the possible future increase in water demand for agriculture, a possible solution would be to consider less water consuming crops. The implication of excess water abstractions during drought and low flow periods would reduce river flows, possibly below the minimum environmental limit. Alternatively, restrictions on abstraction to maintain the minimum environmental flows may restrict crop yields and food (or energy) production.

4.3. Impact of Land Use Changes on Water Resources

Increasing the broadleaf forest area would result in decreasing streamflow and groundwater recharge due to the increase of soil moisture deficit, more specifically during the spring and summer seasons when plants are at maximum growth rate, taking up a large amount of water and transpiring at maximum rate. Urban expansion could result in increased streamflow (likely to increase in flood risk). Decreasing winter barley and grass areas and increasing the area of oil seed rape would result in

increase in soil moisture deficit and a slight decrease in river flow as the crop is expected to take up more water during the spring season where the maximum growth takes place. The impact of the land use changes on the water resources was much less than the effect of climate change. However, considering the possible changes in climatic and extreme events in the future, sustainable land use practices could potentially be used to mitigate the impact of climate change on the catchment's water supplies.

5. Conclusions

- The DiCaSM model calibration and validation results showed a good agreement between the observed simulated flow and overall model efficiency; the NSE index was above 82% for the 51-year study period.
- In addition to the streamflow, the model identified all drought events using the drought indices: SPI, RDI, SMD and the WI, especially in the 1970s, but also during the 1980s, 1990s and most recently the drought in 2010–2012. The analysis revealed that the adjusted RDI index, based on net rainfall (excluding interception losses by vegetation cover) and actual evapotranspiration, was successful in identifying the past drought events and their severity levels. Under climate change projection, the streamflow and the groundwater recharge significantly decreased, especially during the summer, and the severity of the drought events significantly increased.
- All the applied drought indices (SMD, WI and RDI) identified an increase in the severity of the drought under future climatic scenarios. Under high emission scenarios, the drought severity was higher. These findings help in planning for perhaps extra water infrastructure work if needed, such as building more reservoirs or water transfer pipelines from water-rich to water-poor regions and planning to meet the irrigation water demand under different climatic conditions.
- Increasing the broadleaf forest area could result in decreasing streamflow and groundwater recharge during the spring and summer. Urban expansion could result in increased surface runoff. Decreasing crops, like winter barley and grass areas and increasing oil seed rape area, would result in an increase in soil moisture deficit and a slight decrease in river flow. Impact of the land use changes on the water resources was much less than the effect of climate change. However, sustainable land use practices could potentially be used to mitigate the impact of climate change on the catchment's water supplies. Generally, the findings from the modelling work can be used to review the surface water abstraction regulations, as the hydrological model proved to be a good tool to predict river flow and recharge to groundwater and is capable at simulating the effects of climate change on the different elements of the hydrological cycle.

Author Contributions: M.A. was responsible for the model application and analysis of the results. R.R. is the project leader and responsible for the model development.

Funding: The authors acknowledge the NERC funding for this 4-years “Drought Risk and You, DRY” project, grant reference NE/L010292/1.

Acknowledgments: We are also very thankful to our CEH colleagues especially Yan Weigang, Egon Dumont, Virginie Keller and James Blake who helped us in preparing the soil model input data. The authors are also very thankful to Lindsey McEwen who helped in organising Local Advisory Group meetings for the Frome catchment. The authors would like to acknowledge the data sources: Background mapping from Ordnance Survey (‘1:250,000 Scale Colour Raster’). Catchment boundary and gauging station location data from Centre for Ecology and Hydrology [18,19]. River and waterbody data from Centre for Ecology and Hydrology (‘Digital Rivers 50km GB’ Web Map Service). Land cover data from Centre for Ecology and Hydrology (Land Cover Map 2007 (25 m raster, GB) Web Map Service [22]). Standardized Precipitation Index time series for IHU groups (1961–2012) [SPI_IHU_groups] data licensed from NERC Centre for Ecology & Hydrology. Soils data courtesy of Cranfield University (1:250,000 Soilscales for England and Wales Web Map Service). Hydrogeology data from British Geological Survey (DiGMapGB 1:625,000 scale digital hydrogeological data).

Conflicts of Interest: The authors declare no conflict of interest

References

1. Wang, H.; Tetzlaff, D.; Soulsby, C. Modelling the effects of land cover and climate change on soil water partitioning in a boreal headwater catchment. *J. Hydrol.* **2018**, *558*, 520–531. [\[CrossRef\]](#)
2. Van Loon, A.; Laaha, G. Hydrological drought severity explained by climate and catchment characteristics. *J. Hydrol.* **2015**, *526*, 3–14. [\[CrossRef\]](#)
3. Byakatonda, J.; Parida, B.; Moalafhi, D.; Kenabatho, P.K. Analysis of long term drought severity characteristics and trends across semiarid Botswana using two drought indices. *Atmos. Res.* **2018**, *213*, 492–508. [\[CrossRef\]](#)
4. Marsh, T.J.; Monkhouse, R.A. Drought in the United Kingdom, 1988–92. *Weather* **1993**, *48*, 15–22. [\[CrossRef\]](#)
5. Marsh, T. The 1995 UK Drought-A Signal of Climatic Instability? Technical Note. *Proc. Inst. Civ. Eng. Water Marit. Energy* **1996**, *118*, 189–195. [\[CrossRef\]](#)
6. Marsh, T.; Cole, G.; Wilby, R. Major droughts in England and Wales, 1800–2006. *Weather* **2007**, *62*, 87–93. [\[CrossRef\]](#)
7. Taylor, V.; Chappells, H.; Medd, W.; Trentmann, F. Drought is normal: The socio-technical evolution of drought and water demand in England and Wales, 1893–2006. *J. Hist. Geogr.* **2009**, *35*, 568–591. [\[CrossRef\]](#)
8. Kendon, M.; Marsh, T.; Parry, S. The 2010–2012 drought in England and Wales. *Weather* **2013**, *68*, 88–95. [\[CrossRef\]](#)
9. Hulme, M.; Jenkins, G.J.; Lu, X.; Turnpenny, J.R.; Mitchell, T.D.; Jones, R.G.; Lowe, J.; Murphy, J.M.; Hassell, D.; Boorman, P.; et al. *Climate Change Scenarios for the United Kingdom: The UKCIP02 Scientific Report*; Tyndall Centre for Climate Change Research, School of Environmental Sciences, University of East Anglia: Norwich, UK, 2002; 120p.
10. Macdonald, A.M.; Robins, N.S.; Ball, D.F.; Dochartaigh, B.É.Ó. An overview of groundwater in Scotland. *Scott. J. Geol.* **2005**, *41*, 3–11. [\[CrossRef\]](#)
11. Bryant, S.; Arnell, N.; Law, F. The long-term context for the current hydrological drought. In Proceedings of the IWEM Conference on the Management of Scarce water Resources, Brighton, UK, 13–14 October 1992.
12. Jones, P.; Conway, D.; Briffa, K. *Precipitation Variability and Drought*; Routledge: London, UK, 1997.
13. Phillips, I.D.; McGregor, G.R. The utility of a drought index for assessing the drought hazard in Devon and Cornwall, South West England. *Meteorol. Appl.* **1998**, *5*, 359–372. [\[CrossRef\]](#)
14. Fowler, H.; Kilsby, C.; Fowler, H.; Kilsby, C. A weather-type approach to analysing water resource drought in the Yorkshire region from 1881 to 1998. *J. Hydrol.* **2002**, *262*, 177–192. [\[CrossRef\]](#)
15. Charlton, M.B.; Bowes, M.J.; Hutchins, M.G.; Orr, H.G.; Soley, R.; Davison, P. Mapping eutrophication risk from climate change: Future phosphorus concentrations in English rivers. *Sci. Total Environ.* **2018**, *613*, 1510–1526. [\[CrossRef\]](#) [\[PubMed\]](#)
16. Robinson, E.; Blyth, E.; Clark, D.; Comyn-Platt, E.; Finch, J.; Rudd, A. *Climate Hydrology and Ecology Research Support System Potential Evapotranspiration Dataset for Great Britain (1961–2015) [CHESS-PE]*; NERC Environmental Information Data Centre: Lancaster, UK, 2015.
17. Tanguy, M.; Dixon, H.; Prosdociimi, I.; Morris, D.G.; Keller, V.D.J. *Gridded Estimates of Daily and Monthly Areal Rainfall for the United Kingdom (1890–2015) [CEH-GEAR]*; NERC Environmental Information Data Centre: Lancaster, UK, 2016.
18. Morris, D.; Flavin, R.; Moore, R. A digital terrain model for hydrology. In Proceedings of the 4th International Symposium on Spatial Data Handling, Zurich, Switzerland, 23–27 July 1990.
19. Morris, D.; Flavin, R. *Sub-Set of the UK 50 M by 50 M Hydrological Digital Terrain Model Grids*; NERC, Institute of Hydrology: Wallingford, UK, 1994.
20. NRFA. National River Flow Archive. 2014. Available online: <http://nrfa.ceh.ac.uk/> (accessed on 1 November 2014).
21. CEH. CEH Digital River Network of Great Britain Web Map Service. 2014. Available online: <https://data.gov.uk/dataset/3c7ea82e-83e0-45a3f-8ba653b3211b/ceh-digital-river-network-of-great-britain-web-map-service> (accessed on 1 November 2014).
22. Morton, D.; Rowland, C.; Wood, C.; Meek, L.; Marston, C.; Smith, G.; Wadsworth, R.; Simpson, I. *Final Report for LCM2007-The New UK land Cover Map*; Countryside Survey Technical Report No. 11/07; NERC Centre for Ecology & Hydrology: Lancaster, UK, 2011.
23. Ragab, R.; Bromley, J. IHMS-Integrated Hydrological Modelling System. Part1 Hydrological processes and general structure. *Hydrol. Process.* **2010**, *24*, 2663–2680. [\[CrossRef\]](#)

24. Ragab, R.; Bromley, J.; Dörflinger, G.; Katsikides, S. IHMS-Integrated Hydrological Modelling System. Part2 Application of linked unsaturated, DiCaSM and saturated zone, MODFLOW models on Kouris and Akrotiri catchments in Cyprus. *Hydrol. Process.* **2010**, *24*, 2681–2692. [\[CrossRef\]](#)
25. Nash, J.; Sutcliffe, J. River flow forecasting through conceptual models part I—A discussion of principles. *J. Hydrol.* **1970**, *10*, 282–290. [\[CrossRef\]](#)
26. Gupta, H.V.; Kling, H.; Yilmaz, K.K.; Martinez, G.F. Decomposition of the mean squared error and NSE performance criteria: Implications for improving hydrological modelling. *J. Hydrol.* **2009**, *377*, 80–91. [\[CrossRef\]](#)
27. Allen, R.G.; Pereira, L.S.; Raes, D.; Smith, M. *Crop Evapotranspiration-Guidelines for Computing Crop Water Requirements-Fao Irrigation and Drainage Paper 56*; FAO: Rome, Italy, 1998; Volume 300, p. D05109.
28. Jenkins, G.; Murphy, J.; Sexton, D.; Lowe, J.; Jones, P.; Kilsbu, C. *Ukcp09 Briefing Report*; UK Climate Projections; Met Office Hadley Centre: Exeter, UK, 2009.
29. Cloke, H.L.; Jeffers, C.; Wetterhall, F.; Byrne, T.; Lowe, J.; Pappenberger, F. Climate impacts on river flow: Projections for the Medway catchment, UK, with UKCP09 and CATCHMOD. *Hydrol. Process.* **2010**, *24*, 3476–3489. [\[CrossRef\]](#)
30. Ledbetter, R.; Prudhomme, C.; Arnell, N. A method for incorporating climate variability in climate change impact assessments: Sensitivity of river flows in the Eden catchment to precipitation scenarios. *Clim. Chang.* **2012**, *113*, 803–823. [\[CrossRef\]](#)
31. Bastola, S.; Murphy, C.; Fealy, R. Generating probabilistic estimates of hydrological response for Irish catchments using a weather generator and probabilistic climate change scenarios. *Hydrol. Process.* **2012**, *26*, 2307–2321. [\[CrossRef\]](#)
32. Gudmundsson, L.; Bremnes, J.B.; Haugen, J.E.; Engen-Skaugen, T. Technical Note: Downscaling RCM precipitation to the station scale using statistical transformations—A comparison of methods. *Hydrol. Earth Syst. Sci.* **2012**, *16*, 3383–3390. [\[CrossRef\]](#)
33. Wang, L.; Chen, W. A CMIP5 multimodel projection of future temperature, precipitation, and climatological drought in China. *Int. J. Climatol.* **2014**, *34*, 2059–2078. [\[CrossRef\]](#)
34. McKee, T.B.; Doesken, N.J.; Kleist, J. The relationship of drought frequency and duration to time scales. In Proceedings of the 8th Conference on Applied Climatology, Anaheim, CA, USA, 17–22 January 1993; American Meteorological Society: Boston, MA, USA, 1993.
35. Tsakiris, G.; Pangalou, D.; Vangelis, H. Regional drought assessment based on the Reconnaissance Drought Index (RDI). *Water Resour. Manag.* **2007**, *21*, 821–833. [\[CrossRef\]](#)
36. Vangelis, H.; Tigkas, D.; Tsakiris, G. The effect of PET method on Reconnaissance Drought Index (RDI) calculation. *J. Arid Environ.* **2013**, *88*, 130–140. [\[CrossRef\]](#)
37. Zarch, M.A.A.; Sivakumar, B.; Sharma, A. Droughts in a warming climate: A global assessment of Standardized precipitation index (SPI) and Reconnaissance drought index (RDI). *J. Hydrol.* **2015**, *526*, 183–195. [\[CrossRef\]](#)
38. Michaelides, S.; Pashiardis, S. Monitoring drought in Cyprus during the 2007–2008 hydrometeorological year by using the standardized precipitation index (SPI). *Eur. Water* **2008**, *23*, 123–131.
39. Livada, I.; Assimakopoulos, V. Spatial and temporal analysis of drought in Greece using the Standardized Precipitation Index (SPI). *Theor. Appl. Climatol.* **2007**, *89*, 143–153. [\[CrossRef\]](#)
40. Karavitis, C.A.; Tsemlis, D.E.; Skondras, N.A.; Stamatakis, D.; Alexandris, S.; Fassouli, V.; Vasilakou, C.G.; Oikonomou, P.; Gregorič, G.; Grigg, N.S.; et al. Linking drought characteristics to impacts on a spatial and temporal scale. *Hydrol. Res.* **2014**, *16*, 1172–1197. [\[CrossRef\]](#)
41. Al-Faraj, F.A.; Scholz, M.; Tigkas, D.; Boni, M. Drought indices supporting drought management in transboundary watersheds subject to climate alterations. *Water Policy* **2014**, *17*, 865–886. [\[CrossRef\]](#)
42. Herrera-Pantoja, M.; Hiscock, K. The effects of climate change on potential groundwater recharge in Great Britain. *Hydrol. Process.* **2008**, *22*, 73–86. [\[CrossRef\]](#)
43. Alexander, L.V.; Tett, S.F.B.; Jónsson, T. Recent observed changes in severe storms over the United Kingdom and Iceland. *Geophys. Res. Lett.* **2005**, *32*. [\[CrossRef\]](#)
44. Charlton, M.B.; Arnell, N.W. Assessing the impacts of climate change on river flows in England using the UKCP09 climate change projections. *J. Hydrol.* **2014**, *519*, 1723–1738. [\[CrossRef\]](#)
45. Gosling, R. Assessing the impact of projected climate change on drought vulnerability in Scotland. *Hydrol. Res.* **2014**, *45*, 806–816. [\[CrossRef\]](#)

46. Kay, A.; Bell, V.A.; Blyth, E.M.; Crooks, S.M.; Davies, H.N.; Reynard, N.S.; Kay, A.; Bell, V. A hydrological perspective on evaporation: Historical trends and future projections in Britain. *J. Water Clim. Chang.* **2013**, *4*, 193–208. [[CrossRef](#)]
47. Chun, K.P.; Wheeler, H.S.; Onof, C. Projecting and hindcasting potential evaporation for the UK between 1950 and 2099. *Clim. Chang.* **2012**, *113*, 639–661. [[CrossRef](#)]
48. Khalili, D.; Farnoud, T.; Jamshidi, H.; Kamgar-Haghighi, A.A.; Zand-Parsa, S. Comparability Analyses of the SPI and RDI Meteorological Drought Indices in Different Climatic Zones. *Water Resour. Manag.* **2011**, *25*, 1737–1757. [[CrossRef](#)]



© 2019 by the authors. Licensee MDPI, Basel, Switzerland. This article is an open access article distributed under the terms and conditions of the Creative Commons Attribution (CC BY) license (<http://creativecommons.org/licenses/by/4.0/>).